www.sciencemag.org/content/345/6193/216/suppl/DC1

Supplementary Materials for

Ex vivo culture of circulating breast tumor cells for individualized testing of drug susceptibility

Min Yu, Aditya Bardia, Nicola Aceto, Francesca Bersani, Marissa W. Madden, Maria C. Donaldson, Rushil Desai, Huili Zhu, Valentine Comaills, Zongli Zheng, Ben S. Wittner, Petar Stojanov, Elena Brachtel, Dennis Sgroi, Ravi Kapur, Toshihiro Shioda, David T. Ting, Sridhar Ramaswamy, Gad Getz, A. John Iafrate, Cyril Benes, Mehmet Toner, Shyamala Maheswaran,* Daniel A. Haber*

*Corresponding author. E-mail: maheswaran@helix.mgh.harvard.edu (S.M.); haber@helix.mgh.harvard.edu (D.A.H.)

Published 11 July 2014, *Science* **345**, 216 (2014)
DOI: 10.1126/science.1253533

This PDF file includes:

Material and Methods

Blood processing through the CTC-iChip

After obtaining informed consent, up to 20 mL of whole blood was collected by venipuncture into two EDTA vacutainer tubes as per IRB protocol (05-300) at the Massachusetts General Hospital. The two tubes of blood were then pooled and a complete blood count was performed using a Sysmex KX blood analyzer. Biotinylated anti-CD45 (R&D) and anti-CD66 (AbD Serotec) antibodies were added at 50fg and 37.5 fg per white blood cell, respectively, to the blood and allowed to incubate on an Invitrogen HulaMixer for 20-30 minutes with a combination of orbital and reciprocal rotation. Avidin-conjugated Dynabeads were prepared weekly by washing three times with 0.01% Tween-20 in PBS and three times with 0.1% BSA in PBS. Dynabeads were added at 125 beads per white blood cell to the blood and incubated for 20 minutes on the HulaMixer.

Inertial focusing devices (IFDs) were manufactured both on site at the MGH Cancer Center/BioMEMs Resource Facility and by Eerie (Erie Scientific LLC, NH). Deterministic lateral displacement (DLD) devices were manufactured by Silex (Silex Microsystems AB, Sweden). (*27*)

Whole blood (6-18 mL) was processed through the CTC-iChip as previously described (*3*). Briefly, blood was processed using a pressure-driven system in which equal air pressure (16-20 psi) was exerted on the buffer (1% Kolliphor P 188) and the blood sample. In the first portion of the iChip, buffer and blood were mixed and debulked, using deterministic lateral displacement (DLD), to remove red blood cells, platelets, and other small blood components into a syringe. The DLD waste syringe was filled at a constant rate of 600 ul per minute with a New Era Pump Systems Inc syringe pump. The DLD product, including magnetically labeled white blood cells, buffer, and circulating tumor cells, entered the CTC iChip, where cells were aligned into single-file by inertial focusing. The aligned cells then passed through microfluidic magnetophoresis,

where the magnetically labeled white blood cells were separated from unlabeled cells, including CTCs, which were collected in suspension as product.

CTC culture and viral infection

CTC cultures were grown in ultralow attachment plates (Corning) containing tumor sphere medium consisting of RPMI-1640 medium (with phenol red) supplemented with EGF (20ng/ml), basic FGF (20ng/ml), B27 (10ml), and 1x Antibiotic-antimycotic (Life Technologies). Cells were cultured in a humid 37^{o}C incubator with 5% CO2 and 4% O2. Culture media were changed every 3-4 days under microscopic monitoring of cell clusters. Culture conditions that were tried but were unsuccessful include the following: (a) MCF10A medium (DMEM/F12, 5% horse serum, 20ng/ml EGF, 0.5ug/ml hydrocortisone, 10ug/ml insulin, 100ng/ml cholera toxin, 1% pen/strep)(*7*). (b) MCF10A medium including Matrigel (BD Bioscience) (*7*). (c) Mammary Epithelial cell Growth Medium (MEGM^{TM}, Lonza). (d) Previously described primary mammary epithelial cells culture medium (*6*). (e) Combined fibroblast feeder layer with a Rho kinase inhibitor (Y-27632) (*4*). (f) Recently described normal stem cell medium (*5*).

Breast cancer cell lines were purchased from ATCC and maintained according to ATCC protocols.

For viral infection, stable Luc-GFP-CTC lines expressing both luciferase and Green Fluorescent Protein (GFP) were generated using high titer lentivirus (Lenti Luc-GFP) as previously described (*28*). Briefly, 100-200x10^5 cells were transduced with concentrated virus (Lenti-X Concentrator, Clontech) along with 8 mg/mL Polybrene (Sigma), and the medium was changed 12 h after infection.

Next generation sequencing analysis of genomic DNA for mutation identification

Hybrid-capture-based next generation library construction was performed using 250ng of double stranded DNA as starting material. DNA was sheared to a size of approximately 130bp with sonication (Covaris, Inc., Woburn, MA) and ligated with Illumina-compatible sequencing adaptors (Elim BioPharma, Hayward, CA). Bead-based capture was performed with a set of oligonucleotides to capture approximately 1000 known cancer genes (RightOn Cancer Sequencing Kit, developed in collaboration with Elim BioPharma). Libraries were normalized using qPCR (Kapa Illumina Library Quantification Kit, Kapa Biosystems, Wilmington, MA), and sequenced on an Illumina HiSeq 2000 sequencer (Illumina, Inc., San Diego, CA). Sequences were aligned with BWA software, and variants called with MuTect software (*29*).

RNA amplification at single cell resolution

RNA samples extracted from CTCs were thawed on ice and incubated at 70°C for 90 seconds. To generate cDNA, samples were treated with reverse transcription master mix (0.05 uL RNase inhibitor, 0.07uL T4 gene 32 protein, and 0.33uL SuperScript III Reverse Transcriptase per 1X volume) and incubated on thermocycler at 50°C for 30 minutes and 70°C for 15 minutes. To remove free primers, 1.0uL of EXOSAP mix was added to each sample, which was incubated at 37°C for 30 minutes and inactivated at 80°C for 25 minutes. Next, a 3'-poly-A tail was added to the cDNA in each sample by incubating in master mix (0.6uL 10X PCR Buffer II, 0.36uL 25mM MgCl2, 0.18uL 100mM dATP, 0.3uL Terminal Transferase, 0.3uL RNase H, and 4.26uL H2O per 1X volume) at 37°C for 15 minutes and inactivated at 70°C for 10 minutes. A second strand cDNA was synthesized by dividing each sample into 4 and incubating in master mix (2.2uL 10X High Fidelity PCR Buffer, 1.76uL 2.5mM each dNTP, 0.066uL UP2 Primer at 100uM, 0.88uL 50mM MgSO4, 0.44uL Platinum Taq DNA Polymerase, and 13.654uL H2O per 1X volume) at 95°C for 3 minutes, 50°C for 2 minutes, and 72°C for 10 minutes. PCR amplification (95°C for 3 minutes, 20 cycles of 95°C for 30 seconds, 67°C for 1 minute, and 72°C for 6 minutes 6 seconds) was performed with master mix (4.1uL 10X High Fidelity PCR Buffer, 1.64uL 50mM MgSO4, 4.1uL 2.5mM each dNTP, 0.82uL AUP1 Primer at 100uM, 0.82uL AUP2 Primer at 100uM, 0.82uL Platinum Taq DNA Polymerase, and 6.7uL H2O per 1X volume). The 4

reactions of each sample were pooled and purified using the QIAGEN PCR Purification Kit (Cat. No 28106) and eluted in 50uL EB buffer. Samples were selected by testing for genes Gapdh, ActB, Ptprc (CD45), Krt8, Krt18 and Krt19 using qPCR. Each sample was again divided in 4 and a second round of PCR amplification (9 cycles of 98°C for 3 minutes, 67°C for 1 minute, and 72°C for 6 minutes 6 seconds) was performed with master mix (9uL 10X High Fidelity PCR Buffer, 3.6uL 50mM MgSO4, 13.5uL 2.5mM each dNTP, 0.9uL AUP1 Primer at 100uM, 0.9uL AUP2 Primer at 100uM, 1.8uL Platinum Taq DNA Polymerase, and 59.1uL H2O per 1X volume). Samples were pooled and purified using Agencourt AMPure XP beads and eluted in 40uL 1X low TE buffer.

RNA sequencing library construction and data analysis

To shear the DNA using the Covaris S2 System, 1X low TE buffer and 1.2uL shear buffer were added to each sample. Conditions of the shearing program include: 6 cycles, 5°C bath temperature, 15°C bath temperature limit, 10% duty cycle, intensity of 5, 100 cycles/burst, and 60 seconds. Then, samples were end-polished at room temperature for 30 minutes with a master mix (40uL 5X Reaction Buffer, 8uL 10mM dNTP, 8uL End Polish Enzyme1, 10uL End Polish Enzyme2, and 14uL H2O per 1X volume). DNA fragments larger than 500bp were removed with 0.5X volumes of Agencourt AMPure XP beads. Supernatant was transferred to separate tubes. To size-select 200-500bp DNA products, 0.3X volumes of beads were added and samples were washed twice with 70% EtOH. The products were eluted in 36uL low TE buffer. A dA-tail was added to each size-selected DNA by treating with master mix (10uL 5X Reaction Buffer, 1uL 10mM dATP, and 5uL A-Tailing Enzyme I per 1X volume) and incubated at 68°C for 30 minutes and cooled to room temperature. To label and distinguish each DNA sample for sequencing, barcode adaptors (5500 SOLiD 4464405) were ligated to DNA using the 5500 SOLiD Fragment Library Enzyme Module (4464413). Following barcoding, samples were purified twice using the Agencourt AMPure XP beads and eluted in 22uL low TE buffer. Following a round of PCR Amplification (95°C for 5 minutes, 12 cycles of 95°C for 15 seconds, 62°C for 15 seconds, and 70°C for 1 minute, and 70°C for 5 minutes), the libraries were purified with AMPure XP beads. Finally, to quantify the amount of ligated DNA, SOLiD Library

TaqMan Quantitation Kit was used to perform qPCR. Completed barcoded libraries were then subjected to emulsion PCR with template beads preparation and sequenced on the ABI 5500XL.

Determination of reads-per-million (rpm): All RNA-Seq reads were aligned using tophat and bowtie1 with the no-novel-juncs argument set with human genome version hg19 and transcriptome defined by the hg19 knownGene table from genome.ucsc.edu. Reads that did not align or aligned to multiple locations in the genome were discarded. The hg19 table knownToLocusLink from genome.ucsc.edu was used to map each aligned read with the reads count for each gene divided by the total number of reads and multiplied by one million to generate the reads-per-million (rpm) count.

RNA-Seq reads for uncultured CTCs (GEO GSE51827) and the six cultured CTC lines (GEO GSE55807) were deposited into GEO.

Clustering: The reads-per-million (rpm) counts were log transformed (after adding one to eliminate zeros) and the resulting values were quantile normalized to the quantiles of the established cell lines. The result was then median polished. The rows (corresponding to genes) with the top 2000 standard deviations were retained and the rest of the rows were discarded. The result was clustered using agglomerative hierarchical clustering with average linkage with distance metric equal to 1 minus the Pearson correlation coefficient.

Because it is often the case in single-cell RNA-Seq that many genes have no reads, we modified the single-sample GSEA method described in the methods section of (*30*) to deal with ties as follows. Keeping the terminology of (*30*), let $L = \{r_1, r_2, \cdots, r_N\}$ be ranks of the genes according

to their absolute expression from high to low, but if multiple genes have the same absolute expression, replace all their ranks with the average rank of the genes that have that absolute expression. We let the enrichment score be given by

$$\mathrm{ES}(G,S) = \frac{1}{N}\sum_{i=1}^{N}\left[P_G^w(G,S,i) - P_{N_G}(G,S,i)\right]$$

where

$$P_G^w(G,S,i) = \sum_{r_j \in G, r_j \geq N-i+1} \frac{\left|r_j\right|^\alpha}{\sum_{r_j \in G}\left|r_j\right|^\alpha}$$

and

$$P_{N_G}(G,S,i) = \sum_{r_j \notin G, r_j \geq N-i+1} \frac{1}{(N - N_G)}$$

Mouse xenograft assays

The animal protocol was approved by the MGH Subcommittee on Research Animal Care. Six-week old female NSG (NOD.Cg-Prkdcscid Il2rgtm1Wjl/SzJ) mice (Jackson Laboratory) were anesthetized with isofluorane, 20,000 cells in 100ul of 1:1 PBS and Matrigel (BD) were injected into the 4th right mammary fat pad. For tail vein injection, 6,000 cells in 100 µl PBS solution were injected into the lateral tail vein of the mouse. A 90 day release 0.72mg estrogen pellet (Innovative Research of America) was implanted subcutaneously behind the neck of each mouse. Tumor-derived signals (from luciferase-tagged CTC cell lines) were monitored by *in vivo* live imaging using IVIS Lumina II (PerkinElmer). D-Luciferon substrate (PerkinElmer) was injected

intraperitoneally at 150ul/animal, mice were anesthetized after 5 minutes, and bioluminescent images were taken. For *in vivo* drug sensitivity test, BYL719 (25mg/kg) and AZD4547 (12.5mg/kg) were administrated daily via oral gavage, either as single drug or together as combination therapy in solvent (0.5% sodium carboxymethyl cellulose). Control mice were treated with DMSO in same solvent.

Drug sensitivity assays

All compounds were purchased commercially and used at concentrations shown in the relevant figures. For drugs and drug combinations represented within heatmaps (Figure 2), concentrations are listed in supplementary table 3. Cells were seeded one day prior to treatment in 384-well ultralow attachment black wall microplates in tumor sphere medium at 200 cells per well. Each drug was tested on quadruplicate samples at 5 different concentrations, each representing a 2-fold increase from the previous concentration. The drug concentrations selected were centered on the IC_{50} that we had previously established for each drug across large number of cancer cell lines (*17*). Drugs were re-added after 3 days of the initial treatment and cell viability was assayed after 6 days of drug exposure. Signal from the viable cells remaining after drug treatment was measured using CellTiter-Glo (Promega) according to manufacturers instructions. Cell viability was normalized to corresponding quadruplicate samples treated with vehicle controls.

Antibodies and immunoblot analysis

Antibodies used were directed against the estrogen receptor (Leica), GAPDH (Millipore), IRDye-800 anti-Rabbit (Rockland), IRDye-680 anti-Rabbit (LI-COR). For Western blotting, cells were lysed in RIPA buffer [20mM Tris, pH8/150mM NaCl/10mM NaF/0.1% SDS/1% Nonidet P-40/1x protease inhibitor mixture (Roche)]. Lysates were separated on SDS/4-15% polyacrylamide gels (Bio-Rad) and transferred onto Nitrocellulose membrane (Invitrogen), and immunoblots were visualized and quantified using Odyssey Clx (LI-COR).

Immunofluorescence analysis

CTC lines were spun down onto poly-L-lysine-functionalized glass slides with Spintrap (*27*), fixed with 4% paraformaldehyde and washed with PBS. Fixed cells were then permeabilized with 1% NP40 in PBS, blocked with 2% goat serum/3% BSA, and immunostained with relevant primary antibodies. Primary antibodies for CTC analyses were rabbit wide-spectrum anti-cytokeratin (Abcam), mouse IgG2a anti-CD45 (Abcam), and mouse IgG1 anti-Ki67 (Zymed). The secondary antibodies were goat anti-rabbit Alexa Fluor 647 (Invitrogen), goat anti-mouse IgG2a Alexa Fluor 488 (Invitrogen), and goat anti-mouse IgG1 Alexa Fluor 555 (Invitrogen). Nuclei were stained with DAPI and the cover slips were mounted with VECTASHIELD (Vector lab).

Immunocytochemistry

Slides were incubated in 0.3% hydrogen peroxide in methanol for 20 minutes to block endogenous peroxidase activity. Cells were then permeabilized with 0.2% Triton X-100 in PBS for 10 minutes. Antigen retrieval was performed in 1x citrate buffer (pH 6) for 15 minutes in a pressure cooker at the lowest setting. After the suspension was cooled to room temperature, slides were washed in 0.2% Tween 20 in PBS. Samples were blocked for 30 minutes with 0.2% Tween 20, 5% Goat serum in PBS. Primary ER antibody (Leica ER6F12: ORG-8871) was diluted 1:100 in Dako Antibody diluent and samples were incubated for one hour at room temperature. Following three 0.2% Tween-20 washes and one PBS wash, the slides were incubated with HRP anti-mouse antibody (EnVision+ DAKO) for 30 minutes. After washing with PBS, the peroxidase reaction was performed with 3, 3'-diaminobenzidine (DAB) from Vector lab kits for 10 minutes. Cells were counterstained with Gill's #2 hematoxylin for 10-15 seconds, dehydrated with ethanol and cleared with xylene before mounting with Fisher Scientific Permount mounting medium. Slides were imaged with a Nikon 90-I microscope.

References in Methods:

27. N. M. Karabacak *et al.*, *Nat Protoc* **9**, 694 (Mar, 2014).

28. J. Lee, J. B. Wang, F. Bersani, B. Parekkadan, *Langmuir* **29**, 10611 (Aug 27, 2013).

29. K. Cibulskis *et al.*, *Nat Biotechnol* **31**, 213 (Mar, 2013).

30. D. A. Barbie *et al.*, *Nature* **462**, 108 (Nov 5, 2009).

Supplementary Figure legends

Fig. S1. CTC culture conditions.

A. Phase contrast images of the BRx-33 CTC cell line cultured under adherent conditions in serum-containing media and under non-adherent conditions using sphere media. Scale bar, 100 μm. Cultured CTC cells underwent senescent-like growth arrest when cultured under adherent conditions. **B.** Successful culture of CTCs correlates with increased tumor burden. The graph shows changes in the serum tumor marker CA15-3 over time during therapy for 3 patients (BRx-42, BRx-61, BRx-68) who had serial CTC cultures. The time points at which CTC cultures failed or succeeded are shown in red and green, respectively. (*) Represents a failed BRx-42 culture due to poor depletion of blood components during the CTC-iChip run. (**) Represents two BRx-61 CTC cultures successfully established at two different time points for which tumor marker measurements are not available. The time points at which a new therapy regimen was started and discontinued by the treating oncologist who was blinded to the CTC results are shown in black. The new therapy regimen comprised of paclitaxel plus akt inhibitor for BRx-42, paclitaxel for BRx-61, and fulvestrant plus PI3K inhibitor for BRx-68. The blue bar represents the time window available for *in vitro* drug susceptibility testing of CTC cultures, which could impact choice of next treatment.

Fig. S2. Characterization of cultured CTCs.

A. Images of breast cancer cell lines or white blood cells (WBC) immunostained for cytokeratin (CK, red), Ki67 (yellow), CD45 (green), and DAPI (blue) (left panels), or for ER (brown) using immunohistochemistry. Sections were counterstained with hematoxylin (blue; right panels). These serve as positive and negative controls for the respective stains. Scale bar, 20 μm (left panel) or 10 μm (right panel). **B.** Phase contrast images of cultured CTC lines (left panel, scale bar, 100 μm). Corresponding immunostaining for CK (red), Ki67 (yellow), CD45 (green), and DAPI (blue, scale bar, 20 μm), and immunohistochemical staining for ER (brown) are shown in middle and right panels. Sections were counterstained with hematoxylin (blue; scale bar, 10 μm).

Fig. S3. RNA sequencing of CTC cultures, uncultured CTCs and ATCC breast cancer cell lines

A. Heatmap showing unsupervised hierarchical clustering of transcripts from 6 CTC lines, 29 uncultured CTCs (derived from a total of 10 patients, including patient #10 (BRx-68) and patient #8 (BRx-61)), and 13 commonly used breast cancer cell lines. **B.** Heatmap showing lower proliferation levels of uncultured CTCs compared to CTC cultures or commonly used breast cancer cell lines. **C.** Heatmap showing unsupervised hierarchical clustering of transcripts as in panel "A", but subtracting the cell cycle genes of panel "B".

Fig. S4. Tumorigenicity of CTC lines BRx-07, BRx-61 and BRx-68.

A. Bioluminescence images showing the growth of a xenograft implanted into the mammary fat pad of a NSG mouse, derived from luciferase-tagged BRx-68 CTC cells (left panel). Quantification of bioluminescent signals is shown (right) (n=2). **B.** Hematoxylin & Eosin (H&E) staining of the corresponding primary tumor and xenograft from BRx-68 is shown. Scale bar, 20 μm. **C.** Bioluminescence images showing the growth of a BRx-61 CTC-derived xenograft implanted into the mammary fat pad of a NSG mouse (left panel). Quantification of bioluminescent signals is shown (right) (n=2). **D.** Bioluminescent images showing the growth of BRx-07 CTCs in the lung of a mouse following inoculation via tail vein (left). Quantification of bioluminescent signals is shown (right). **E.** H&E staining of the tumor in the mouse lung (following tail vein CTC cell injection) and the matched metastatic tumor specimen from the same patient. The lower panel shows the corresponding immunohistochemical staining for ER (brown). Specimens were counterstained with hematoxylin. Scale bar, 20 μm.

Fig. S5. Absence of tumor formation using CTC lines BRx-33 and BRx-50.

A. Bioluminescent images showing the absence of sustained proliferation by BRx-33 and BRx-50 CTC lines inoculated into the mammary fat pad (left panels). Quantification of the

bioluminescent signals after inoculation of both cell lines into mice is shown (n=2, right panels). **B.** Patient-derived metastatic tumor (BRx-50) and residual mouse xenograft (lacking growth after 3 months) were stained with H&E (blue) or for ER expression (brown). Scale bar, 20 μm. The residual xenograft tumor cells maintained ER positivity despite a lack of sustained growth.

Fig. S6. Clinical history of breast cancer patients.

Summary of the clinical therapeutic history of patients with metastatic breast cancer whose CTCs were cultured *ex vivo*. Clinical status is listed above the time line bar and treatment regimens are listed below the bar. The time of CTC isolation followed by successful expansion *ex vivo* is shown as red tags on the time line bar.

Fig. S7. Sequence trace showing the *ESR1* mutation identified by RNA sequencing analysis of freshly-isolated single CTCs from patient BRx-68.

Image of the sequence alignment showing an A -> C substitution in location hg19, chr6:152,419,923 in both of the only two reads uniquely aligned to the exon 8 of *ESR1* transcript from uncultured single CTCs freshly isolated from Patient#10 (BRx-68) (Patient#10_SC#1 in GEO GSE51827).

Fig. S8. Heatmaps of drug sensitivity in BRx-42 and BRx-61 lines.

Heatmaps representing the viability of BRx-42 and BRx-61 CTC lines following treatment with a panel of drugs targeting specific pathways, either alone or in combination. Each drug concentration represents a 2-fold increase from the previous dose and each concentration was tested in quadruplicate. Drug concentrations were selected based on IC_{50} from large scale cancer cell line screens (*19*). Signal from the viable cells remaining after drug treatment were normalized to the corresponding samples treated with vehicle control (DMSO) and the ratios were plotted ranging from red (more viable) to blue (less viable).

Fig. S9. Heatmaps of drug sensitivity in MCF7 and MDA-MB-231 breast cancer cell lines.

Heatmaps representing the viability of MCF7 and MDA-MB-231 cells following treatment with a panel of drugs. Each drug concentration represents a 2-fold increase from the previous dose and each concentration was tested in quadruplicate. Drug concentrations were selected based on IC_{50} from large scale cancer cell line screens (*19*). Signal from the viable cells remaining after drug treatment were normalized to the corresponding samples treated with vehicle control (DMSO) and the ratios were plotted ranging from red (more viable) to blue (less viable).

Fig. S10. Dose curves of drug sensitivity in CTC lines.

Dose curves representing the viability of five CTC lines (BRx-07, 68, 50, 42, and 61) following treatment with three drugs (BYL719, AZD4547, and STA9090). Potential relevant mutations in each cell line are shown. Mean±SEM, n=4. Increased sensitivity to PI3K inhibition (BYL719) was evident in three CTC lines harboring a *PIK3CA* mutation (BRx-07, 68, and 42). Sensitivity to the FGFR inhibitor (AZD4547) was evident in BRx-07 (harboring 46% *FGFR2* mutation). BRx-61 CTCs also displayed sensitivity to the FGFR2 inhibitor. Susceptibility to HSP90 inhibitor (STA9090) was evident in BRx-68 (harboring 47% *ESR1* mutation), and BRx-42 (harboring 99% *KRAS* mutation).

Fig. S11. Quantification of responses in breast cancer patients to selected drugs.

Bar graphs showing the duration of drug treatment (in days) in patients BRx-07, BRx-68, and BRx-50 from whom the corresponding CTC cell lines were generated. The treatments were initiated and terminated by the treating oncologists who were blinded to the CTC culture results. As per clinical standards, each therapy is continued for as long as it is potentially effective and hence the duration of treatment is an indicator of clinical efficacy.

Fig. S12. Combinatorial drug treatment analysis.

Heatmaps representing the viability of (**A**) BRx-07, (**B**) BRx-68, (**C**) BRx-50, and (**D**) BRx-50 and BRx-33 cultured CTCs following treatment with drug combinations. Cell viability was normalized to the corresponding vehicle control within each treatment group. Drug concentrations are listed on top or on left and each condition was tested with 8 replicates.

Fig. S13. Quantification of responses in CTC lines to two drug combinations.

Bar graphs representing the viability of BRx-07 and BRx-68 CTC lines following treatment with drug combinations shown. Cell viability was normalized to the corresponding vehicle control within each treatment group. Mean±SEM, n=8. Cooperative drug sensitivity to PI3K inhibition (BYL719) and FGFR inhibitor (AZD4547) was evident in BRx-07 CTC line harboring both *PIK3CA* and *FGFR2* mutations. Increased sensitivity to PI3K inhibition (BYL719) was evident in BRx-68 harboring a *PIK3CA* mutation but there was no cooperative effect with FGFR inhibitor (AZD4547). Cooperative drug sensitivity to HSP90 inhibitor (STA9090) and fulvestrant was evident in BRx-68 (harboring 47% *ESR1* mutation).

Fig. S14. ER expression analysis in BRx-68 and BRx-50 cell lines.

A. The BRx-68 line was immunostained for estrogen receptor expression (brown) at baseline and after 24-hour exposure to fulvestrant or raloxifene, either alone (top panel) or in combination with STA9090 (bottom panel). Sections were counterstained with hematoxylin (blue). Scale bar, 20 μm. **B.** Estrogen receptor expression in the BRx-50 cell line (6% *ESR1* mutation) was analyzed as in panel S14A. DMSO treated control cultures are included. Scale bar, 20 μm**.** The bar graph shows the percentage of estrogen receptor positive cells in the culture under different treatment conditions. More than 200 cells were quantified in each condition. **C.** Immunoblotting for estrogen receptor expression in BRx-50 and BRx-68 cultured CTCs, and in the MCF7 breast cancer cell line following 24 hours of exposure to DMSO (control) or two

concentrations of STA9090. Bar graph shows quantification of estrogen receptor expression normalized to GAPDH and relative to DMSO treated control.

Fig. S15. Combinatorial drug treatment analysis on breast cancer cell lines.

Heatmaps representing the viability of a panel of breast cancer cell lines with *PIK3CA* mutations following combinatorial treatment with AZD4547 and BYL719. Cell viability was normalized to the corresponding vehicle control within each treatment group. Drug concentrations are listed on top or on left and each condition was tested with 8 replicates. When present, mutations of *PIK3CA* and/or *FGFR* are shown in parenthesis. * FGFR2 A1708>G (unknown relevance). **FGFR4 A1100G (unknown relevance).

Table S1. List of the CTC lines.

Table S2. Additional mutations in CTC lines.

Table S3. List of drugs, targeted pathways, and doses.

Figure S1

A

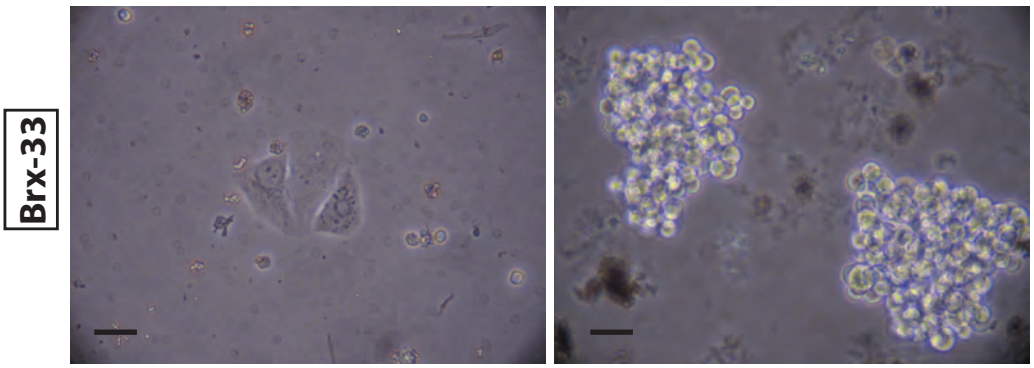
Serum-containing media
Adherent
Sphere media
Non-adherent
Brx-33

B

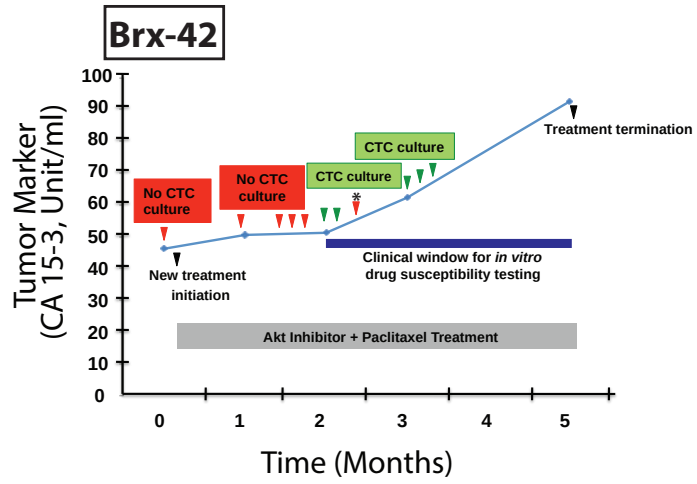
Brx-42
Tumor Marker (CA 15-3, Unit/ml)
Time (Months)
No CTC culture
No CTC culture
CTC culture
CTC culture
Treatment termination
New treatment initiation
Clinical window for in vitro drug susceptibility testing
Akt Inhibitor + Paclitaxel Treatment

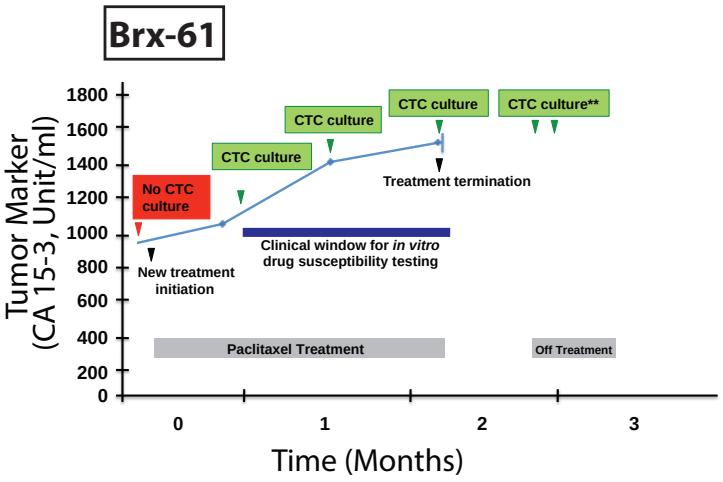
Brx-61
Tumor Marker (CA 15-3, Unit/ml)
Time (Months)
No CTC culture
CTC culture
CTC culture
CTC culture
CTC culture**
Treatment termination
New treatment initiation
Clinical window for in vitro drug susceptibility testing
Paclitaxel Treatment
Off Treatment

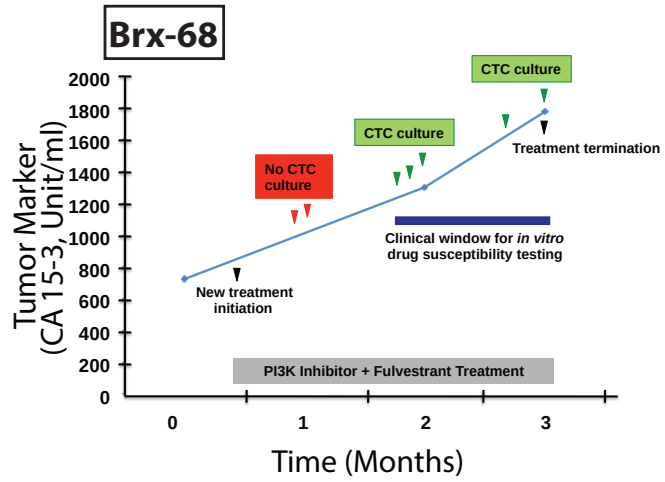
Brx-68
Tumor Marker (CA 15-3, Unit/ml)
Time (Months)
No CTC culture
CTC culture
CTC culture
Treatment termination
New treatment initiation
Clinical window for in vitro drug susceptibility testing
PI3K Inhibitor + Fulvestrant Treatment

Figure S2

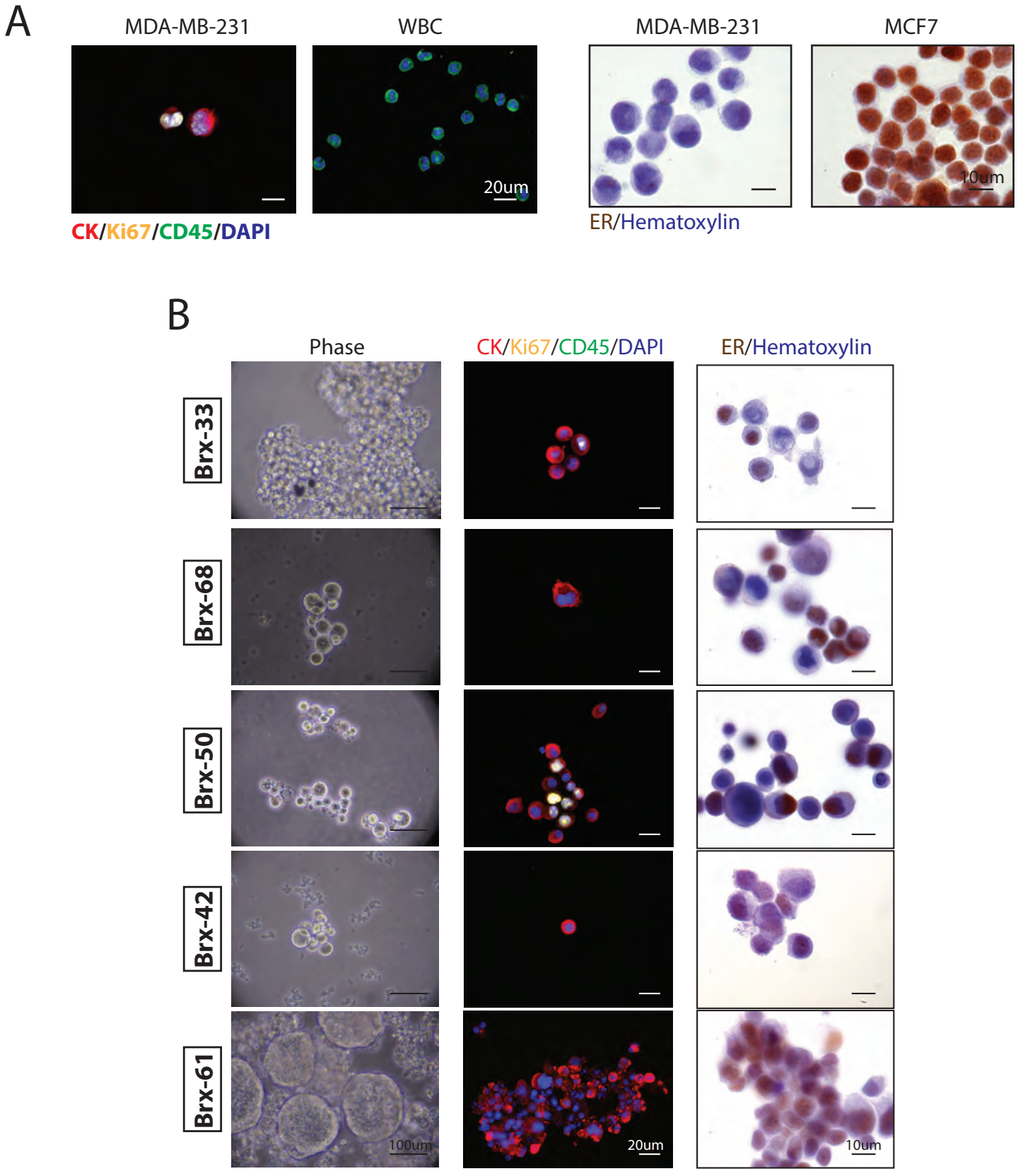
A
MDA-MB-231
WBC
MDA-MB-231
MCF7
20um
10um
CK/Ki67/CD45/DAPI
ER/Hematoxylin
B
Phase
CK/Ki67/CD45/DAPI
ER/Hematoxylin
Brx-33
Brx-68
Brx-50
Brx-42
Brx-61
100um
20um
10um

Figure S3

A

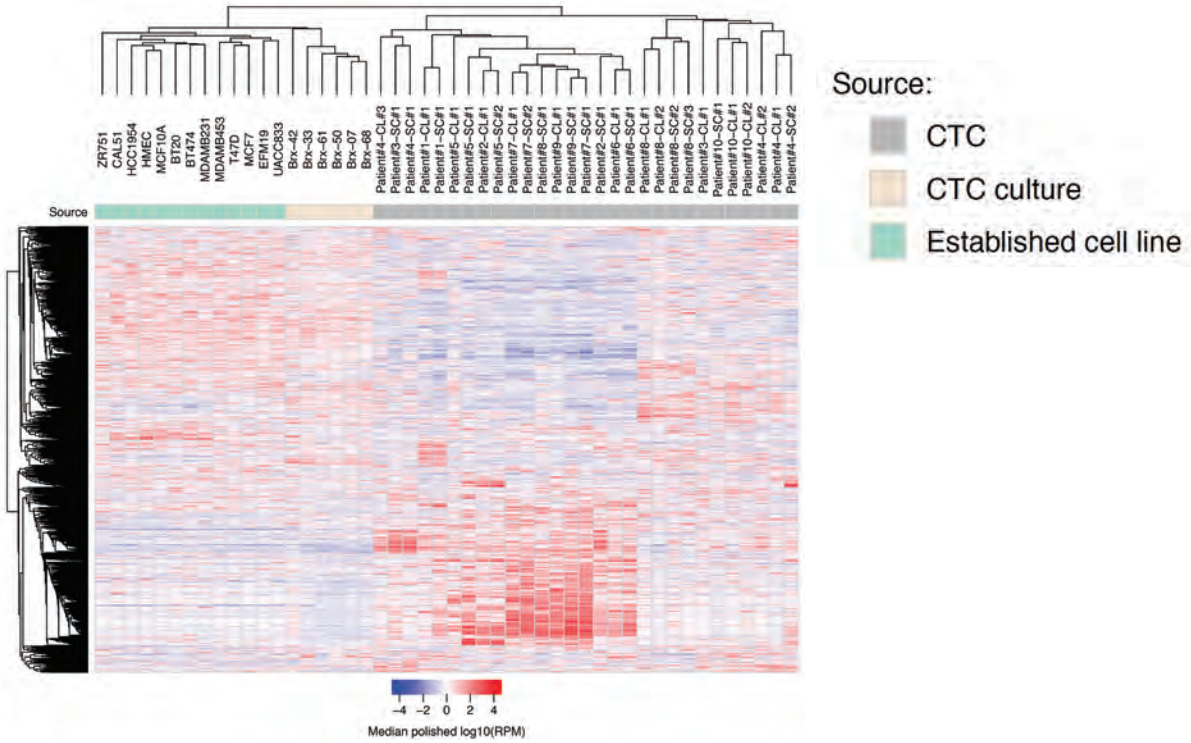

B

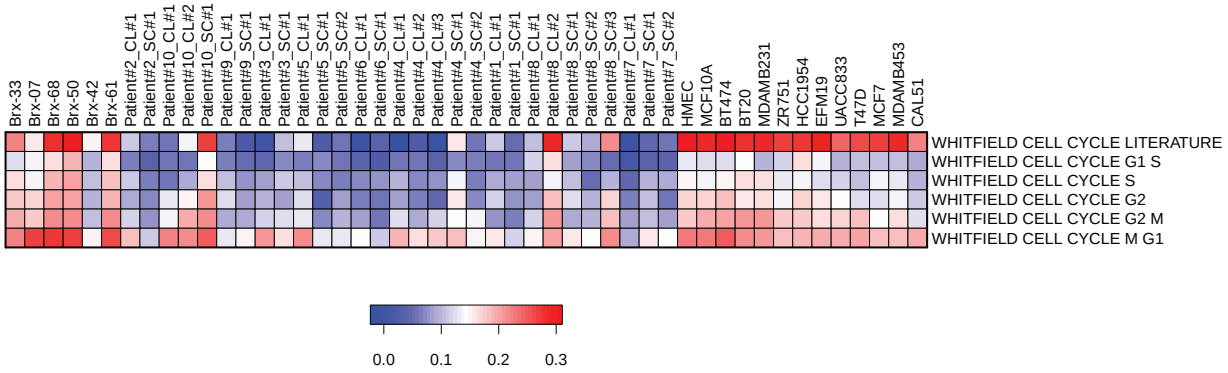

C

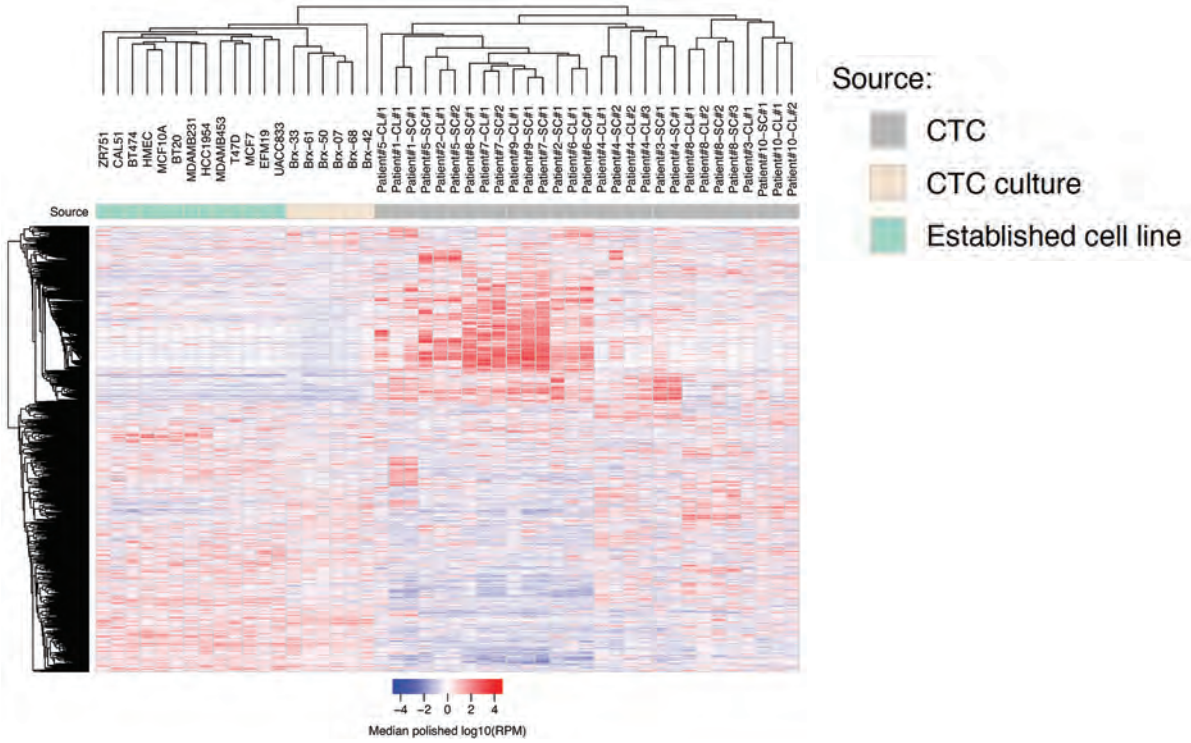

Figure S4

A

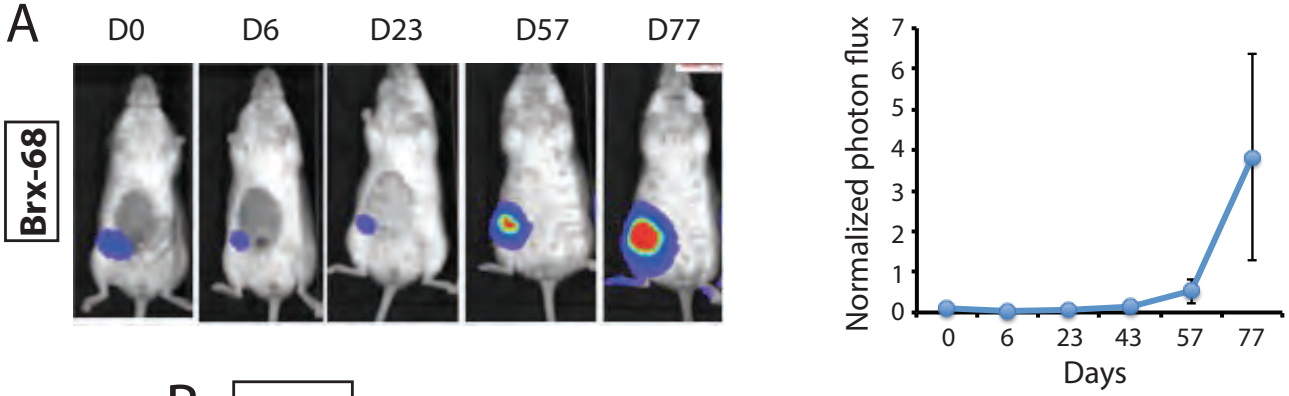

B

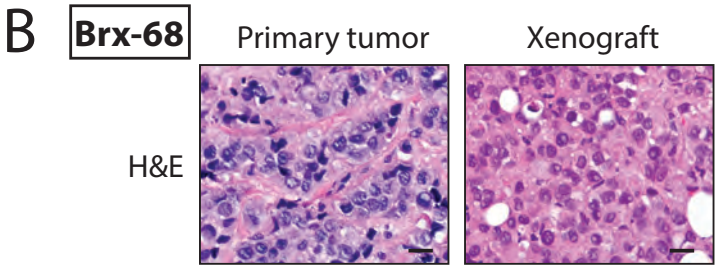

C

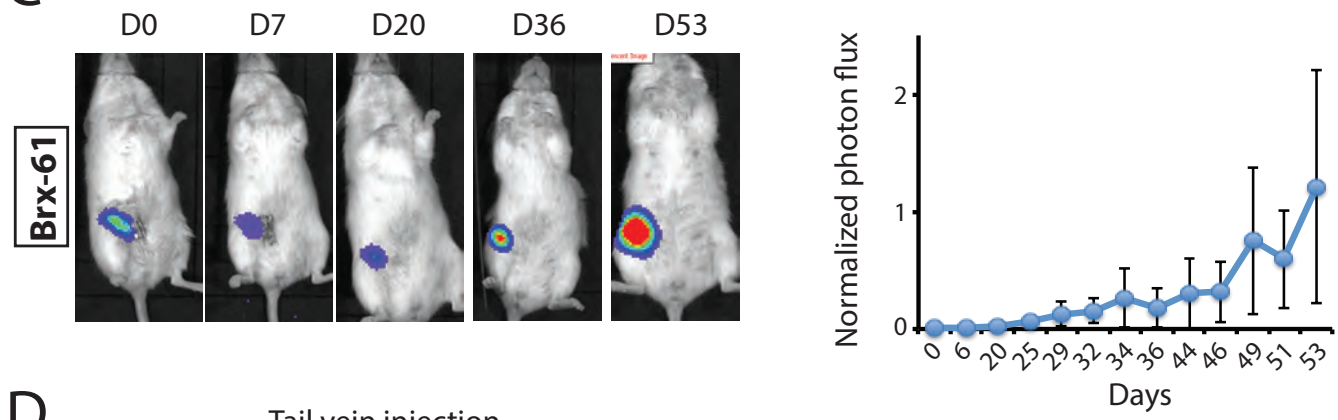

D

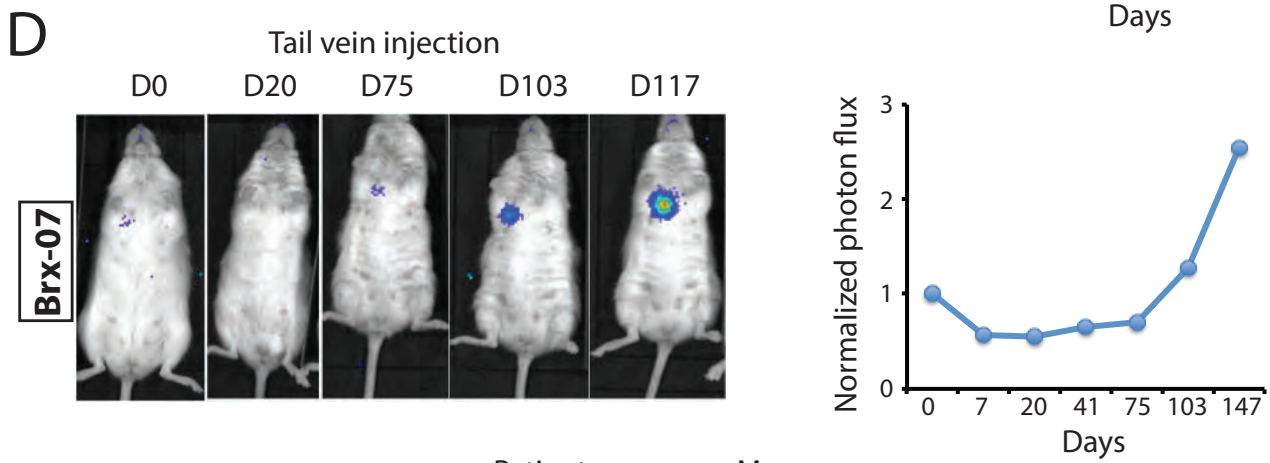

E

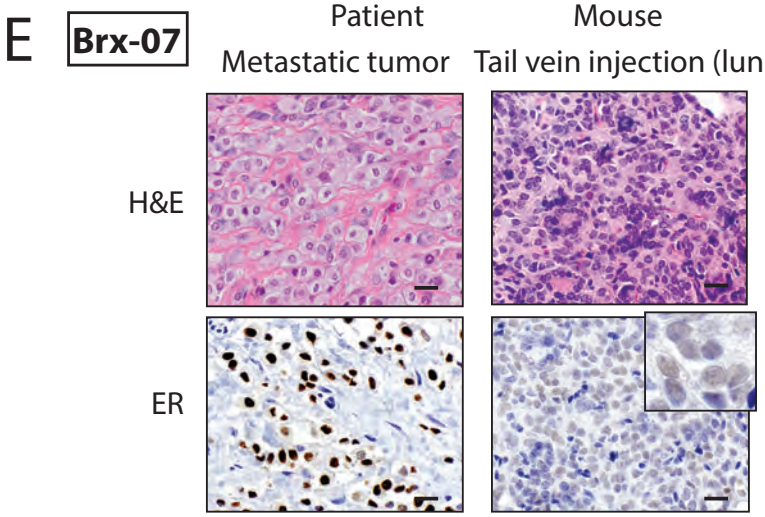

Figure S5

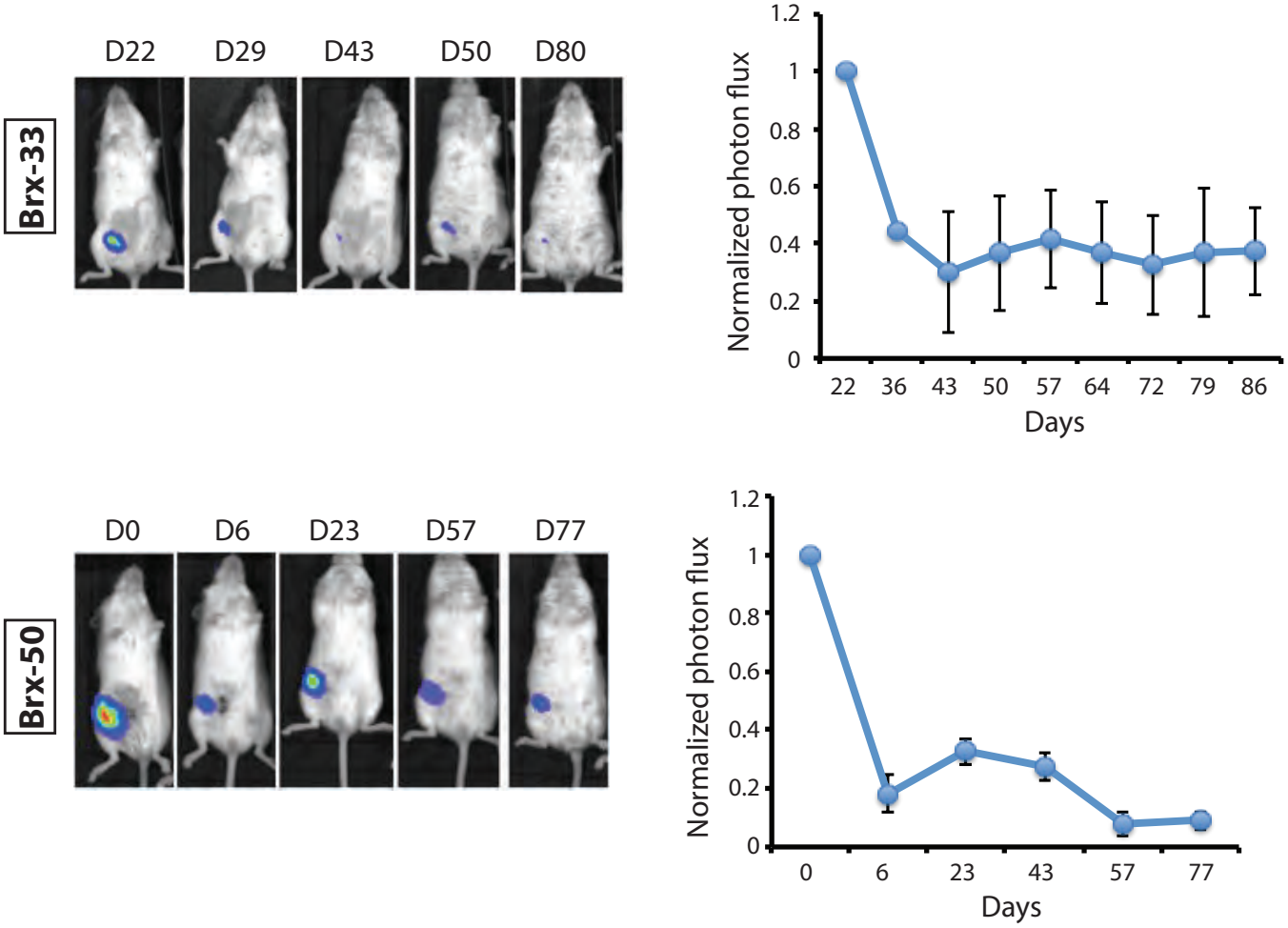
A
Brx-33
D22
D29
D43
D50
D80
Normalized photon flux
1.2
1
0.8
0.6
0.4
0.2
0
22
36
43
50
57
64
72
79
86
Days
Brx-50
D0
D6
D23
D57
D77
Normalized photon flux
1.2
1
0.8
0.6
0.4
0.2
0
0
6
23
43
57
77
Days

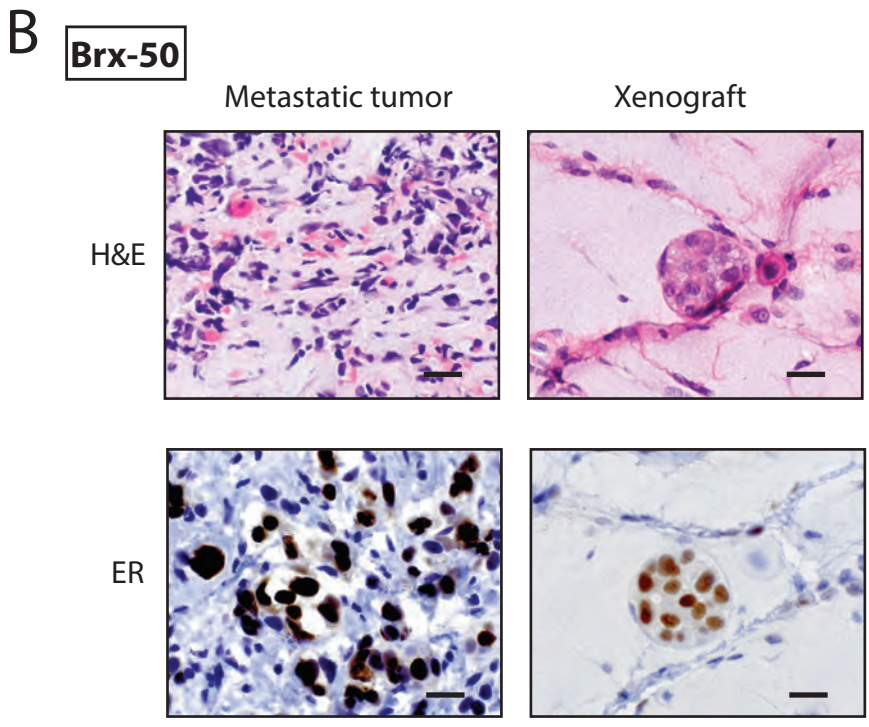
B
Brx-50
Metastatic tumor
Xenograft
H&E
ER

Figure S6

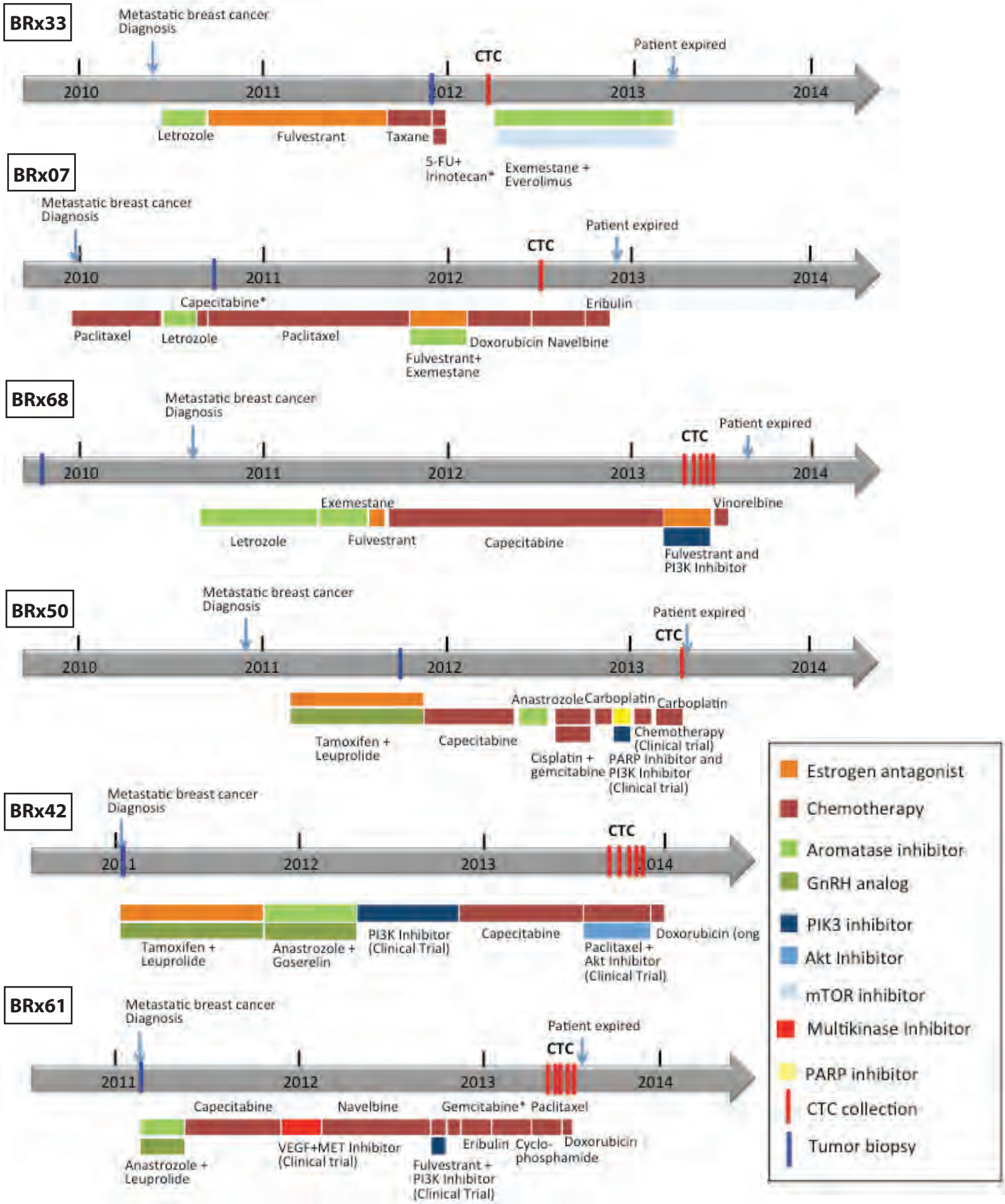
BRx33
Metastatic breast cancer Diagnosis
CTC
Patient expired
2010
2011
2012
2013
2014
Letrozole
Fulvestrant
Taxane
5-FU+ Irinotecan*
Exemestane + Everolimus
BRx07
Metastatic breast cancer Diagnosis
Patient expired
CTC
2010
2011
2012
2013
2014
Capecitabine*
Eribulin
Paclitaxel
Letrozole
Paclitaxel
Doxorubicin
Navelbine
Fulvestrant+ Exemestane
BRx68
Metastatic breast cancer Diagnosis
Patient expired
CTC
2010
2011
2012
2013
2014
Exemestane
Vinorelbine
Letrozole
Fulvestrant
Capecitabine
Fulvestrant and PI3K Inhibitor
BRx50
Metastatic breast cancer Diagnosis
Patient expired
CTC
2010
2011
2012
2013
2014
Anastrozole
Carboplatin
Carboplatin
Tamoxifen + Leuprolide
Capecitabine
Chemotherapy (Clinical trial)
Cisplatin + gemcitabine
PARP Inhibitor and PI3K Inhibitor (Clinical trial)
BRx42
Metastatic breast cancer Diagnosis
CTC
2011
2012
2013
2014
Tamoxifen + Leuprolide
Anastrozole + Goserelin
PI3K Inhibitor (Clinical Trial)
Capecitabine
Doxorubicin (ong
Paclitaxel + Akt Inhibitor (Clinical Trial)
BRx61
Metastatic breast cancer Diagnosis
Patient expired
CTC
2011
2012
2013
2014
Capecitabine
Navelbine
Gemcitabine*
Paclitaxel
Anastrozole + Leuprolide
VEGF+MET Inhibitor (Clinical trial)
Fulvestrant + PI3K Inhibitor (Clinical Trial)
Eribulin
Cyclo-phosphamide
Doxorubicin
Estrogen antagonist
Chemotherapy
Aromatase inhibitor
GnRH analog
PIK3 inhibitor
Akt Inhibitor
mTOR inhibitor
Multikinase Inhibitor
PARP inhibitor
CTC collection
Tumor biopsy

Figure S7

Freshly-isolated single CTC from Patient 10 (Brx-68)

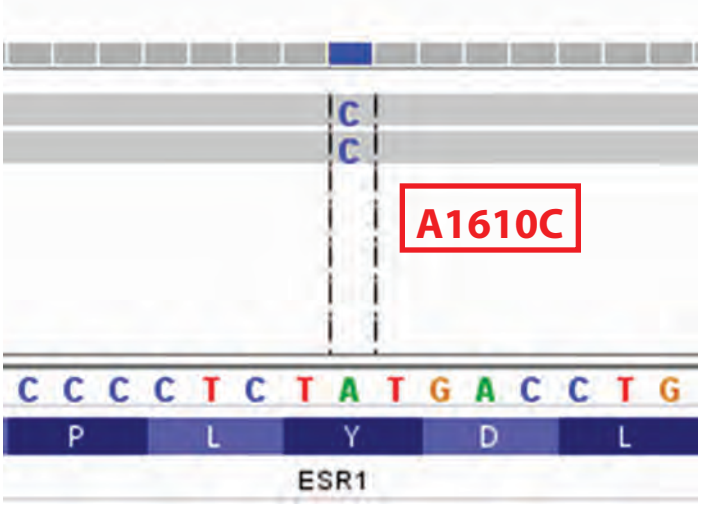

Figure S8

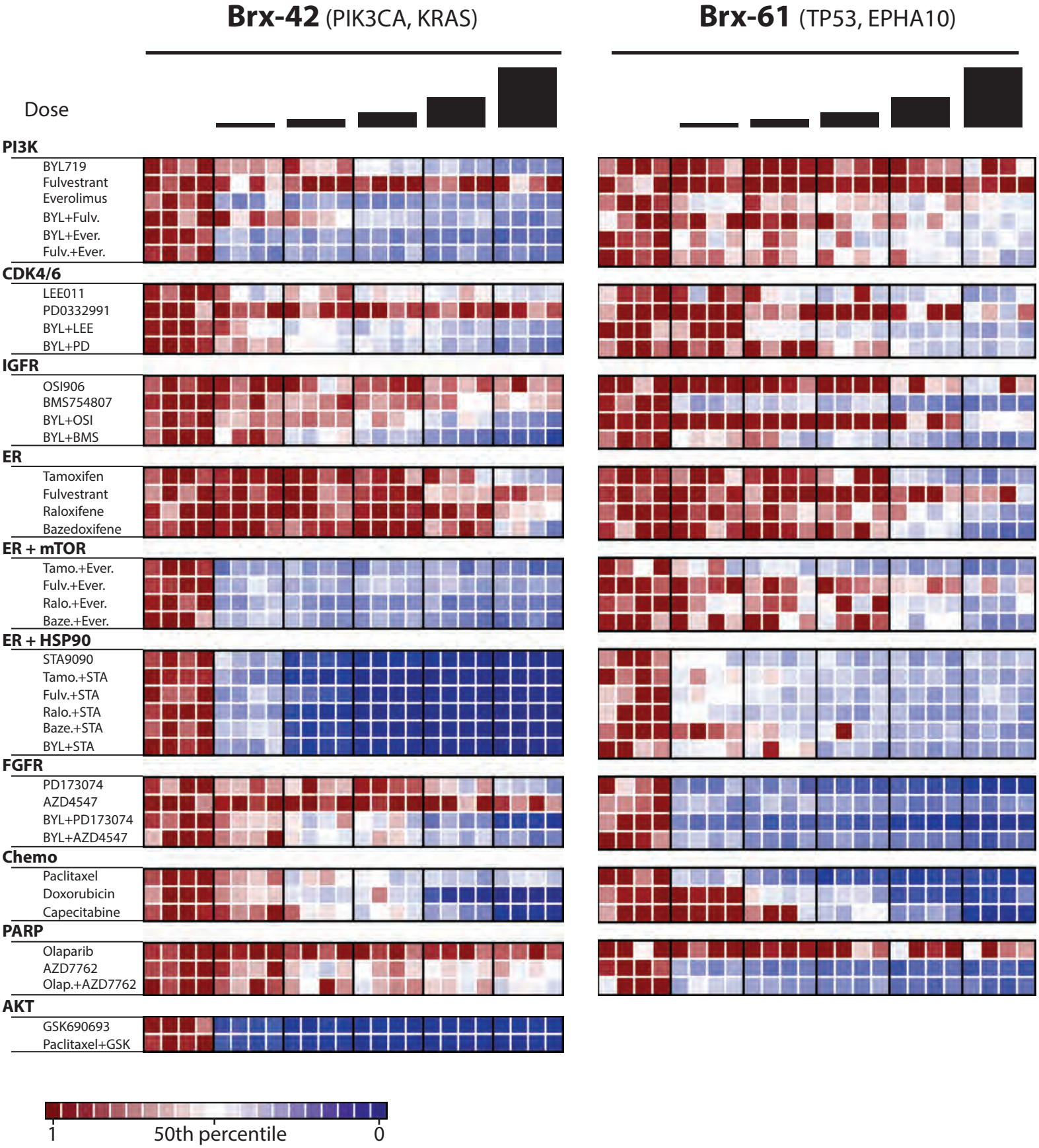
Brx-42 (PIK3CA, KRAS)
Brx-61 (TP53, EPHA10)
Dose
PI3K
BYL719
Fulvestrant
Everolimus
BYL+Fulv.
BYL+Ever.
Fulv.+Ever.
CDK4/6
LEE011
PD0332991
BYL+LEE
BYL+PD
IGFR
OSI906
BMS754807
BYL+OSI
BYL+BMS
ER
Tamoxifen
Fulvestrant
Raloxifene
Bazedoxifene
ER + mTOR
Tamo.+Ever.
Fulv.+Ever.
Ralo.+Ever.
Baze.+Ever.
ER + HSP90
STA9090
Tamo.+STA
Fulv.+STA
Ralo.+STA
Baze.+STA
BYL+STA
FGFR
PD173074
AZD4547
BYL+PD173074
BYL+AZD4547
Chemo
Paclitaxel
Doxorubicin
Capecitabine
PARP
Olaparib
AZD7762
Olap.+AZD7762
AKT
GSK690693
Paclitaxel+GSK
1
50th percentile
0

Figure S9

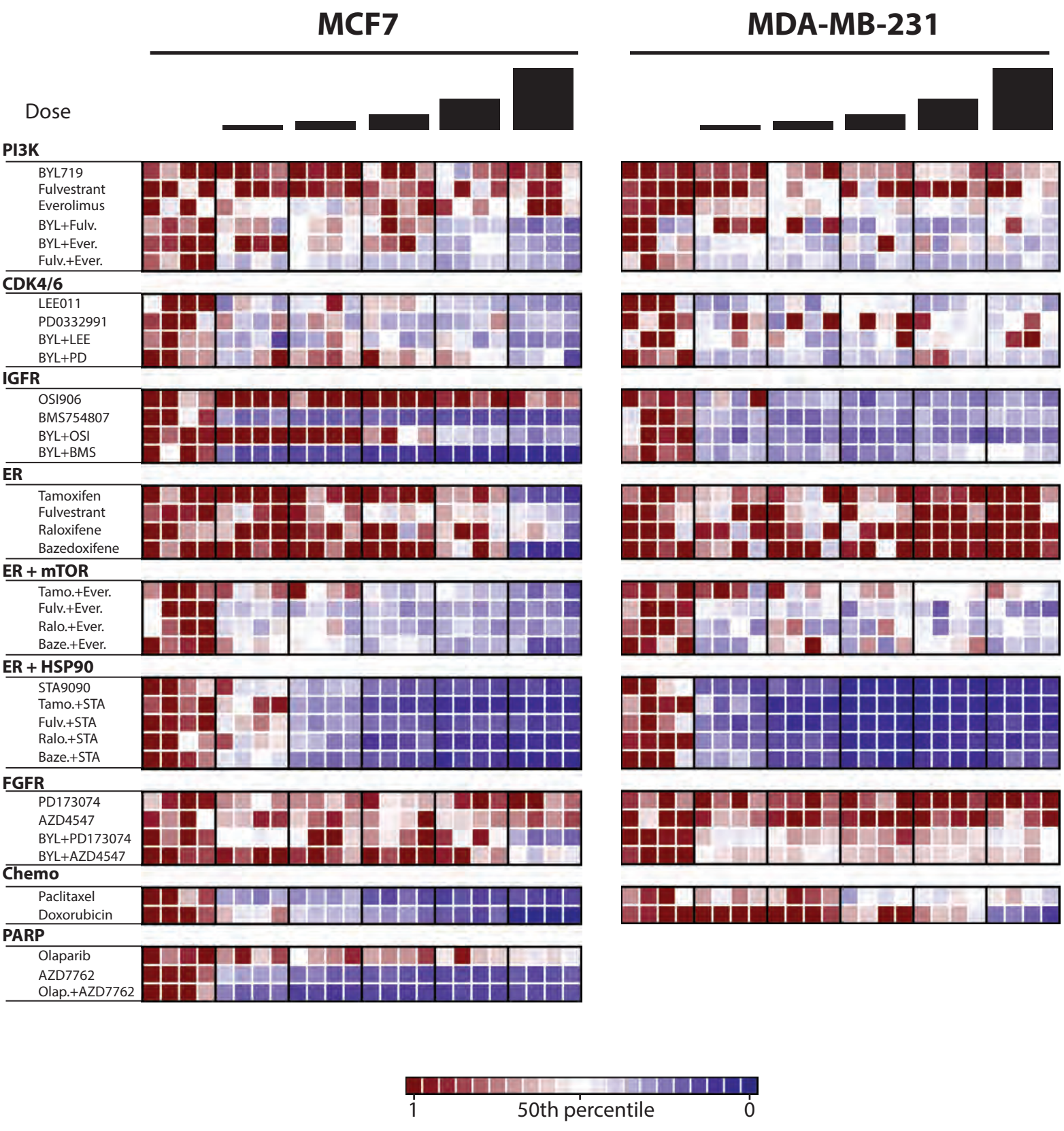
MCF7
MDA-MB-231
Dose
PI3K
BYL719
Fulvestrant
Everolimus
BYL+Fulv.
BYL+Ever.
Fulv.+Ever.
CDK4/6
LEE011
PD0332991
BYL+LEE
BYL+PD
IGFR
OSI906
BMS754807
BYL+OSI
BYL+BMS
ER
Tamoxifen
Fulvestrant
Raloxifene
Bazedoxifene
ER + mTOR
Tamo.+Ever.
Fulv.+Ever.
Ralo.+Ever.
Baze.+Ever.
ER + HSP90
STA9090
Tamo.+STA
Fulv.+STA
Ralo.+STA
Baze.+STA
FGFR
PD173074
AZD4547
BYL+PD173074
BYL+AZD4547
Chemo
Paclitaxel
Doxorubicin
PARP
Olaparib
AZD7762
Olap.+AZD7762
1
50th percentile
0

Figure S10

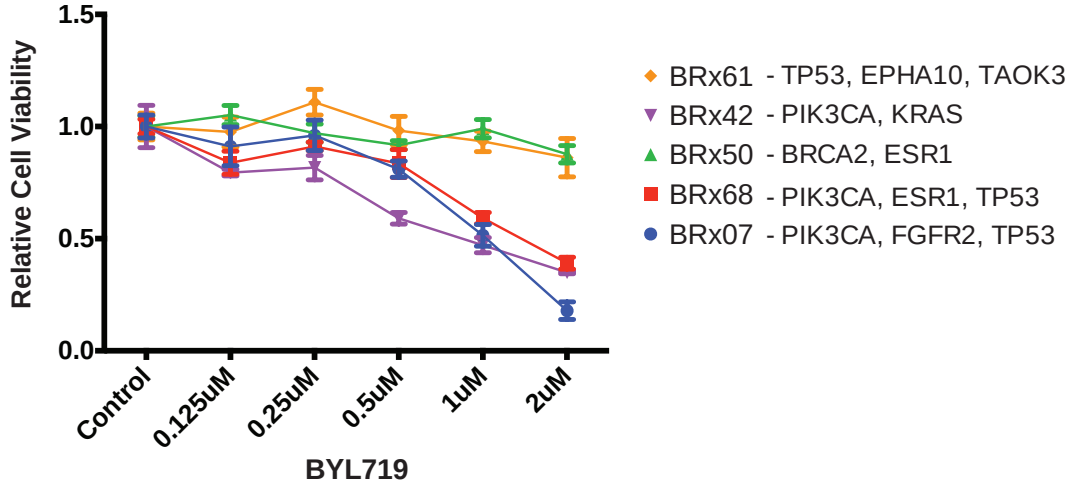
Relative Cell Viability
1.5
1.0
0.5
0.0
Control
0.125uM
0.25uM
0.5uM
1uM
2uM
BYL719
BRx61 - TP53, EPHA10, TAOK3
BRx42 - PIK3CA, KRAS
BRx50 - BRCA2, ESR1
BRx68 - PIK3CA, ESR1, TP53
BRx07 - PIK3CA, FGFR2, TP53

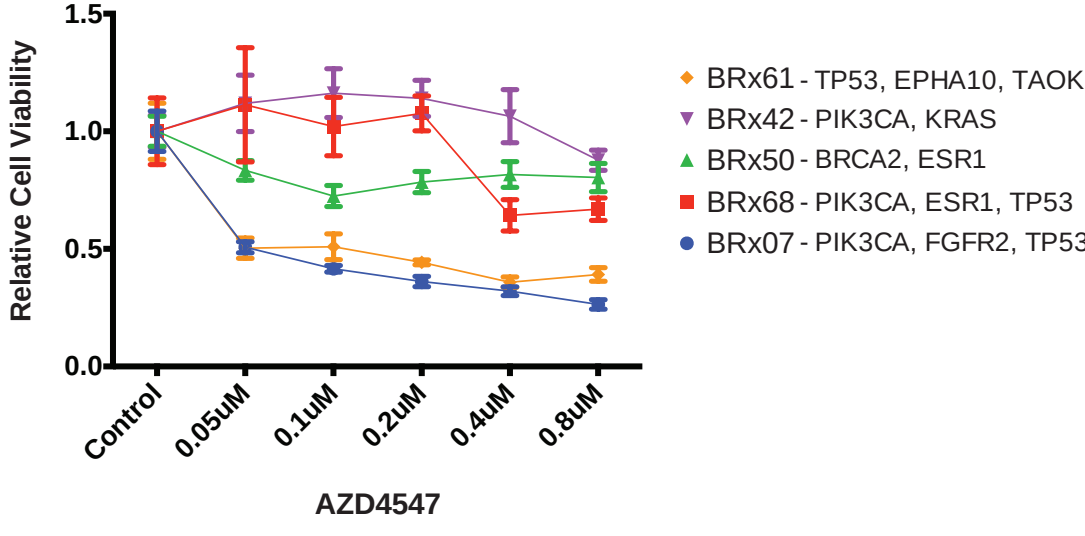
Relative Cell Viability
1.5
1.0
0.5
0.0
Control
0.05uM
0.1uM
0.2uM
0.4uM
0.8uM
AZD4547
BRx61 - TP53, EPHA10, TAOK3
BRx42 - PIK3CA, KRAS
BRx50 - BRCA2, ESR1
BRx68 - PIK3CA, ESR1, TP53
BRx07 - PIK3CA, FGFR2, TP53

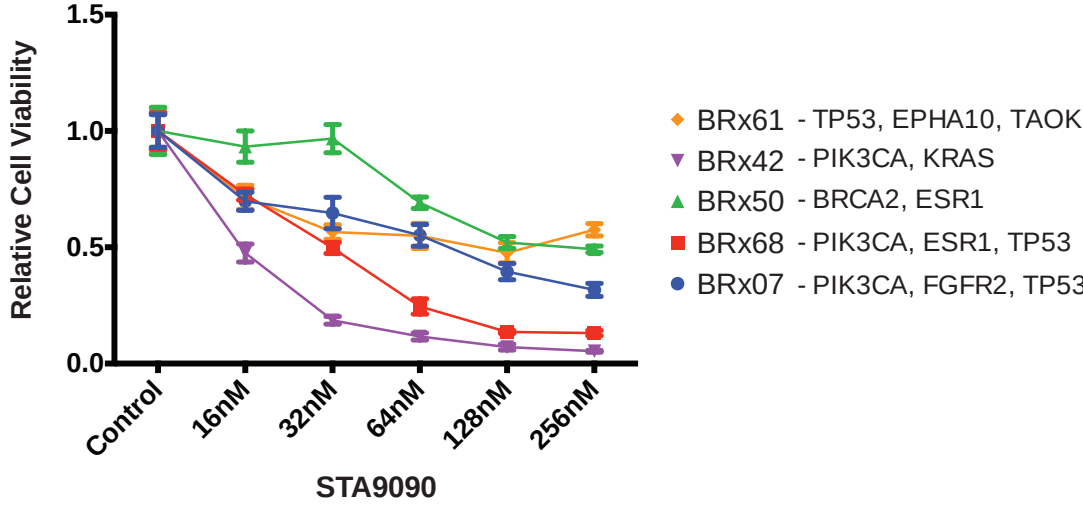
Relative Cell Viability
1.5
1.0
0.5
0.0
Control
16nM
32nM
64nM
128nM
256nM
STA9090
BRx61 - TP53, EPHA10, TAOK3
BRx42 - PIK3CA, KRAS
BRx50 - BRCA2, ESR1
BRx68 - PIK3CA, ESR1, TP53
BRx07 - PIK3CA, FGFR2, TP53

Figure S11

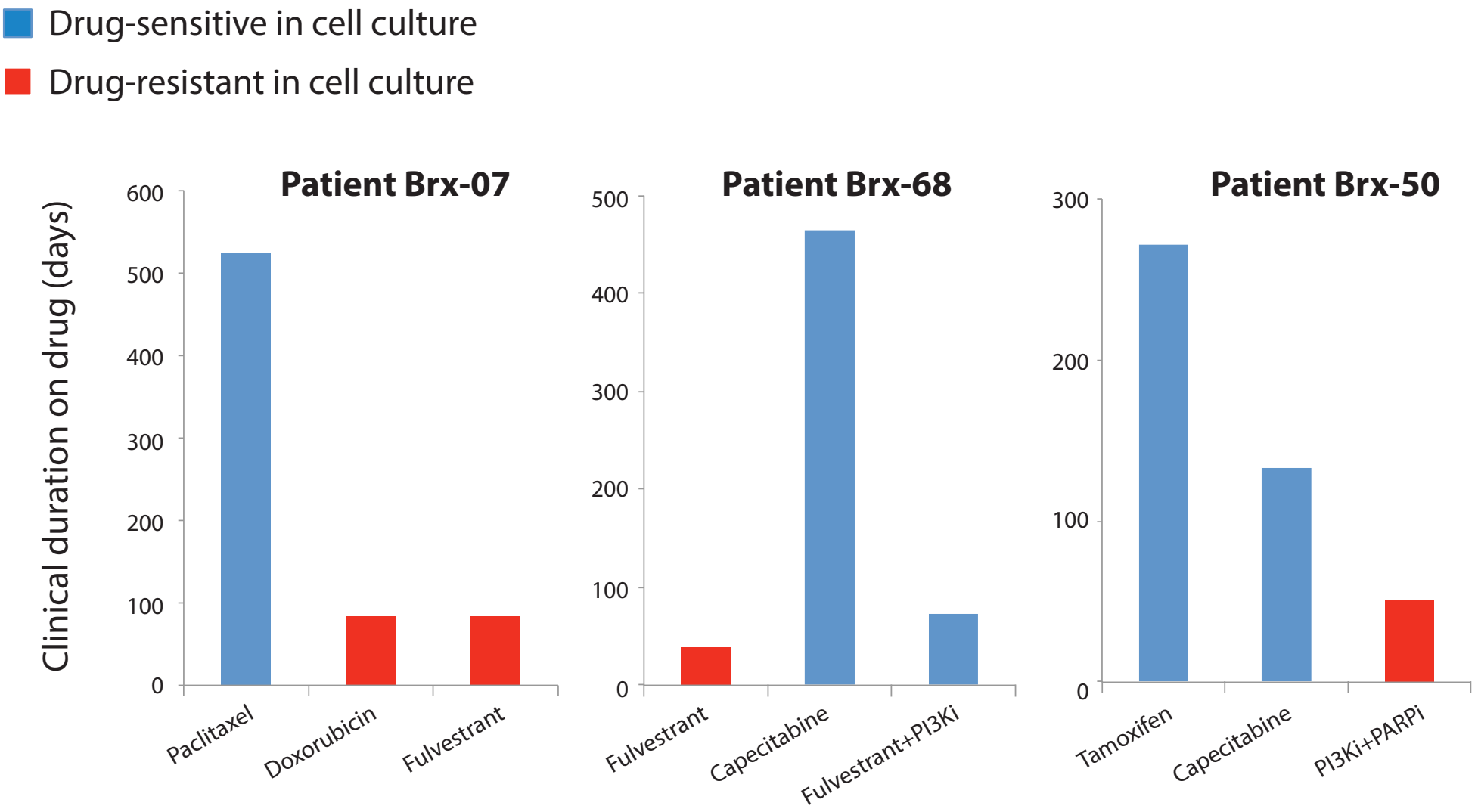
Drug-sensitive in cell culture
Drug-resistant in cell culture
Clinical duration on drug (days)
Patient Brx-07
600
500
400
300
200
100
0
Paclitaxel
Doxorubicin
Fulvestrant
Patient Brx-68
500
400
300
200
100
0
Fulvestrant
Capecitabine
Fulvestrant+PI3Ki
Patient Brx-50
300
200
100
0
Tamoxifen
Capecitabine
PI3Ki+PARPi

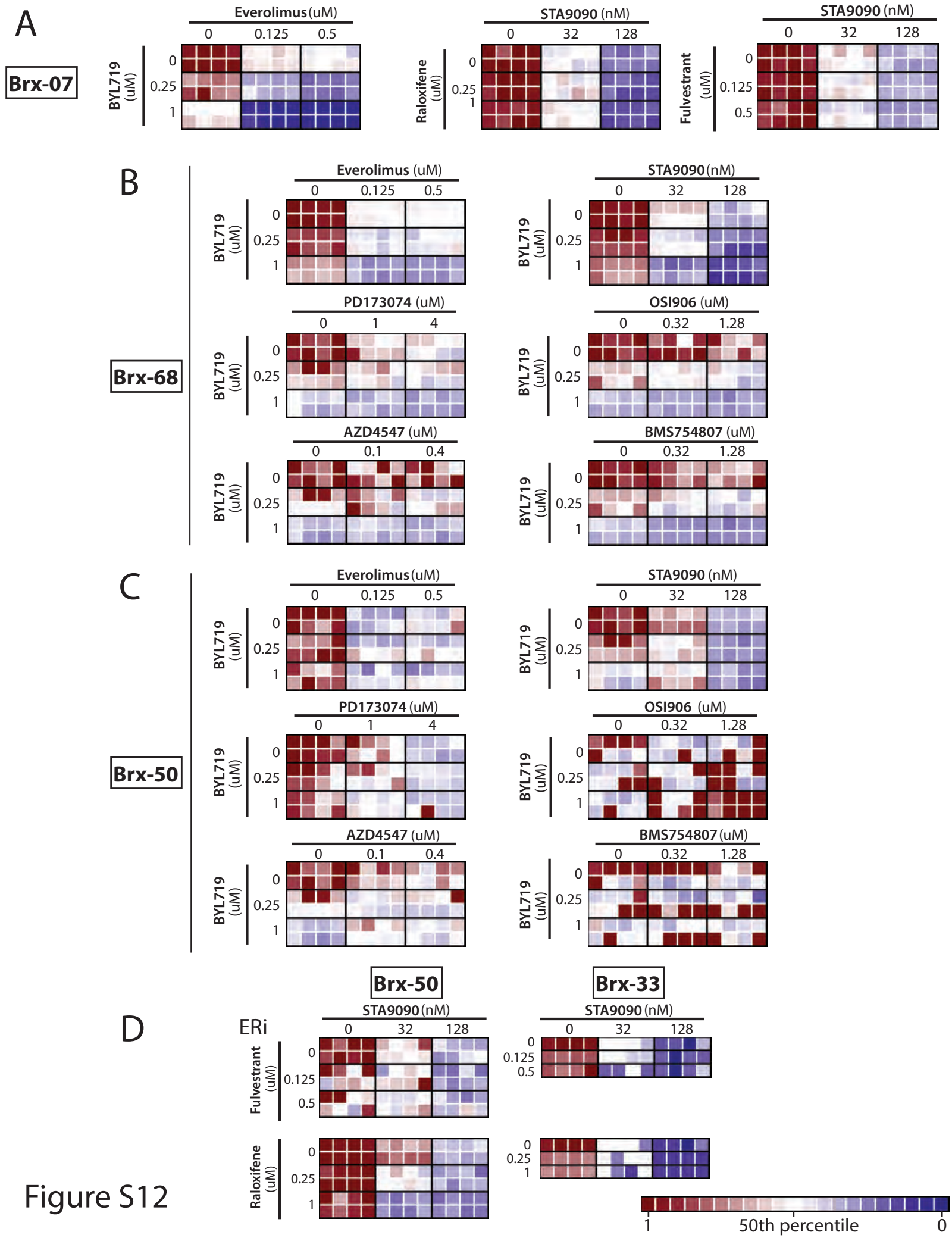
A
Brx-07
Everolimus (uM)
0
0.125
0.5
BYL719 (uM)
0
0.25
1
STA9090 (nM)
0
32
128
Raloxifene (uM)
0
0.25
1
STA9090 (nM)
0
32
128
Fulvestrant (uM)
0
0.125
0.5
B
Brx-68
Everolimus (uM)
0
0.125
0.5
BYL719 (uM)
0
0.25
1
STA9090 (nM)
0
32
128
PD173074 (uM)
0
1
4
OSI906 (uM)
0
0.32
1.28
AZD4547 (uM)
0
0.1
0.4
BMS754807 (uM)
0
0.32
1.28
C
Brx-50
Everolimus (uM)
0
0.125
0.5
STA9090 (nM)
0
32
128
PD173074 (uM)
0
1
4
OSI906 (uM)
0
0.32
1.28
AZD4547 (uM)
0
0.1
0.4
BMS754807 (uM)
0
0.32
1.28
D
ERi
Brx-50
Brx-33
STA9090 (nM)
0
32
128
Fulvestrant (uM)
0
0.125
0.5
Raloxifene (uM)
0
0.25
1
1
50th percentile
0

Figure S12

Figure S13

PI3K+FGFRi

HSP90+ERi

BRx07 (PIK3CA, FGFR2, TP53)

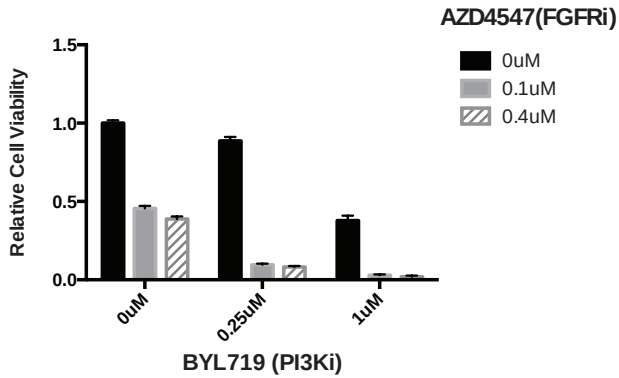

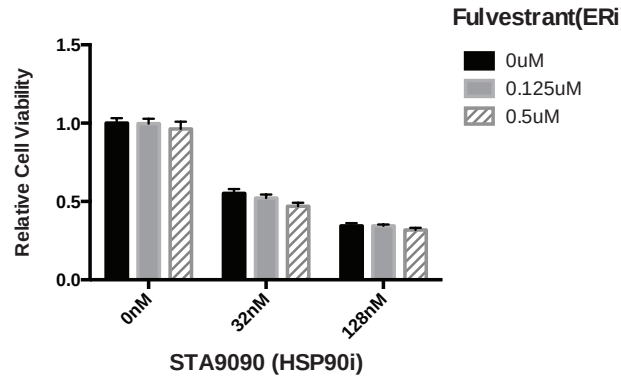

BRx68 (PIK3CA, ESR1, TP53)

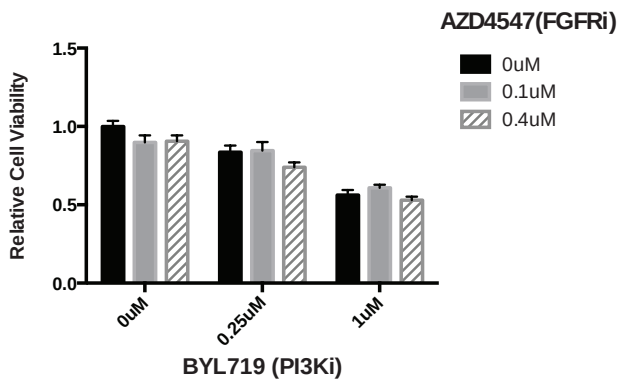

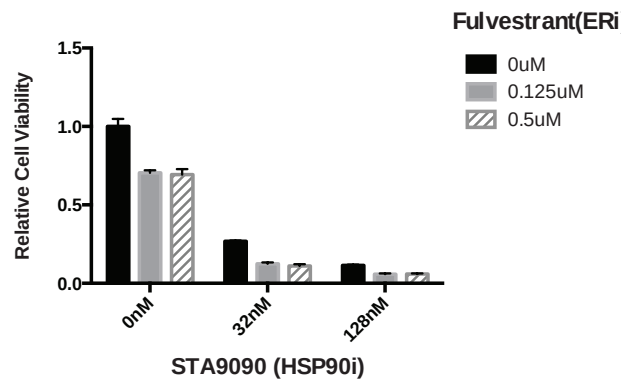

Figure S14

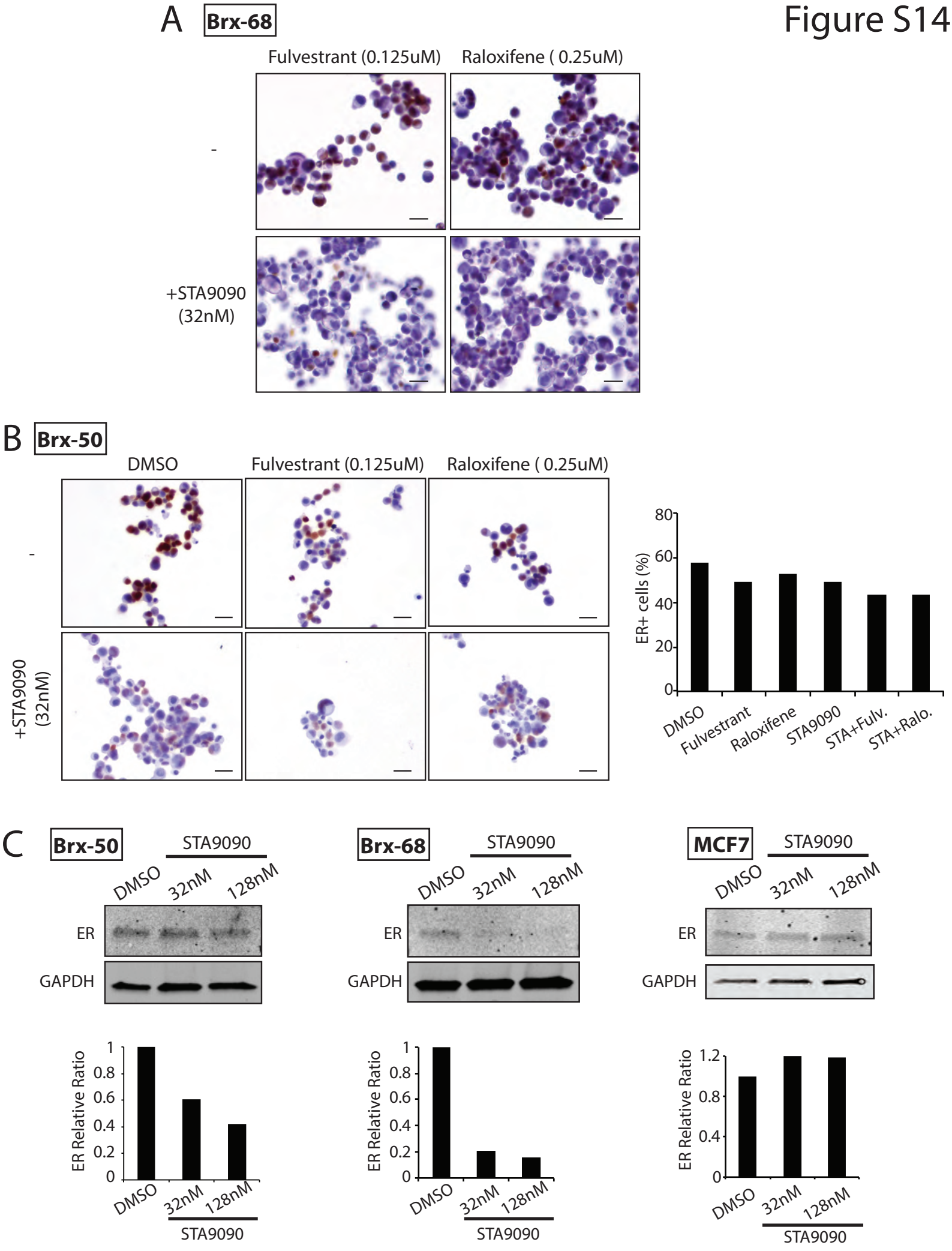
A
Brx-68
Fulvestrant (0.125uM)
Raloxifene (0.25uM)
-
+STA9090
(32nM)
B
Brx-50
DMSO
Fulvestrant (0.125uM)
Raloxifene (0.25uM)
-
+STA9090
(32nM)
ER+ cells (%)
80
60
40
20
0
DMSO
Fulvestrant
Raloxifene
STA9090
STA+Fulv.
STA+Ralo.
C
Brx-50
STA9090
DMSO
32nM
128nM
ER
GAPDH
Brx-68
STA9090
DMSO
32nM
128nM
ER
GAPDH
MCF7
STA9090
DMSO
32nM
128nM
ER
GAPDH
ER Relative Ratio
1
0.8
0.6
0.4
0.2
0
DMSO
32nM
128nM
STA9090
ER Relative Ratio
1
0.8
0.6
0.4
0.2
0
DMSO
32nM
128nM
STA9090
ER Relative Ratio
1.2
0.8
0.4
0
DMSO
32nM
128nM
STA9090

Figure S15

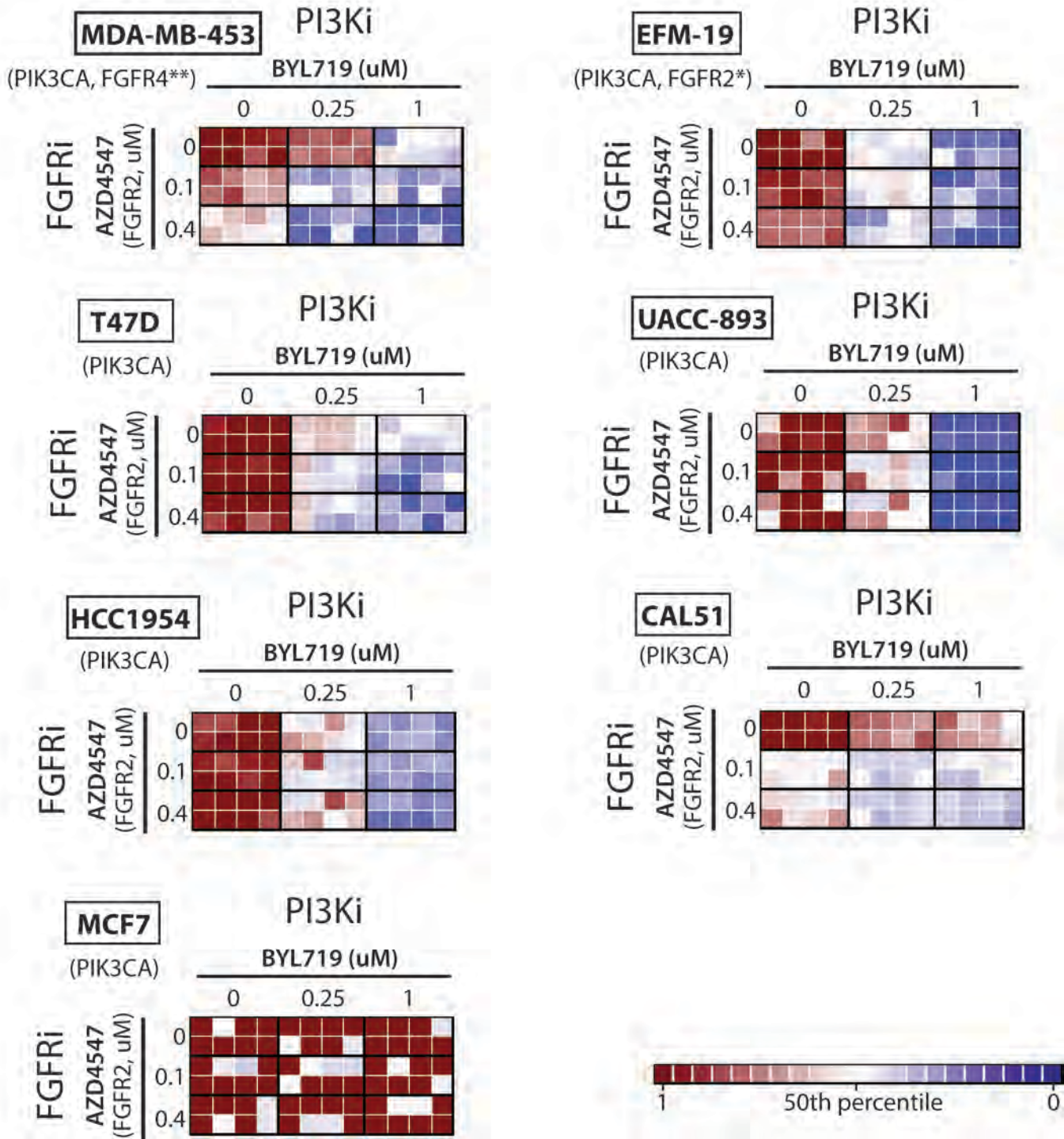
MDA-MB-453
(PIK3CA, FGFR4**)
PI3Ki
BYL719 (uM)
0
0.25
1
FGFRi
AZD4547
(FGFR2, uM)
0
0.1
0.4
EFM-19
(PIK3CA, FGFR2*)
T47D
(PIK3CA)
UACC-893
(PIK3CA)
HCC1954
(PIK3CA)
CAL51
(PIK3CA)
MCF7
(PIK3CA)
1
50th percentile
0

Table S1. List of the CTC lines

Case	Tumor			CTC cell lines				
	Receptor staining (IHC)	Histology	Tumor mutation by SnapShot	Treatment at CTC isolation	# CTCs / 6mls	# of Independent lines	Culture initial doubling time	Total time in culture
BRx-33	ER+/PR+/Her2-	Lobular	none	No	3000	1	3 weeks	>1 year
BRx-07	ER+/PR+/Her2-	Lobular	none	On Eribulin	3	1	1 week	>1 year
BRx-68	ER+/PR+/Her2-	Ductal	PIK3CA	No	50	5	1 week	>9 months
BRx-50[a]	ER+/PR-/Her2-	Ductal	none	No	100	1	3 days	>10 months
BRx-42	ER+/PR+/Her2-	Ductal+Lobular	PIK3CA	On Paclitaxel+AKTi	20	5	2 weeks	>6 months
BRx-61	ER+/PR+/Her2-	Ductal	none	No	50	5	3 weeks	>9 months

a: Patient known to have germline BRCA2 mutation

Table S2. List of additional mutations in cultured CTC lines

Case	Gene	DNA	Protein	Allele[a] Frequency
BRx33[b]	GAK	G3368A	R1123Q	0.51
BRx07[b]	PSCK7	C1876G	Q626E	0.21
	TRIO	A4567G	K1523E	0.14
	TP73	A1208G	Q403R	1
	RNASEL	G1130A	G377E	0.3
	AMER3	G1042A	A348T	0.54
	PDK1	A526C	N176H	0.47
	MAP2K7	C253T	R85C	0.42
	ERRB4	T1627A	F543I	0.5
	L3MBTL3	A2236G	T746A	0.72
	HIP1	184_splice	T62_splice	0.63
	WNK2	C4967T	P1656L	1
	EHMT1	A2695G	I899V	0.32
	MYO3A	T4846C	S1616P	0.54
	NUP98	4009_splice	G1337_splice	0.49
	DDX10	C607T	Q203*	0.49
	KMT2A	G5778A	M1926I	0.47
	PIK3C2G	C205T	P69S	0.43
	NIN	A3611G	Q1204R	0.44
	RPS6KB2	A326G	N109S	0.49
	GSG2	A2116G	M706V	1
	ROCK1	G977A	R326Q	1
	MAP2K7	C253CT	R85C	0.42
BRx68	TIAM1	C4400T	P1467L	0.51
	NTRK1	T20C	I7T	0.3
	CHD1L	C2666G	S889C	0.14
	BCL9	C2183G	S728C	0.02
	DCLK1	C1692T	Y564Y	0.99
	NUTM1	G2052T	L684L	0.23
	TTN	G4307T	R1436I	0.01
	P2RY8	C312T	Y104Y	0.24
	CSNK1A1L	G121A	E41K	0.99
BRx50[b]	IGF2R	G4740C	R1580S	0.99
	TIAM1	C67T	R23C	0.5
	NUP98	C5358G	S1786R	0.47
	NOTCH2	C4261A	P1421T	0.5
	FPGT-TNNI3K,TNNI3K	G712A	A238T	0.47
	NCOA1	C1163A	P388H	0.52
	LRP1B	A3479G	K1160R	0.48
	FEV	G260A	W87*	0.52
	PLAG1	G1126T	A376S	0.48
	FANCG	A500G	N167S	0.47

	IRAK4	C26A	T9K	0.38
	ADAMTSL3	G554C	R185P	0.49
	CIITA	G13A	A5T	0.52
	JAK3	C1207T	R403C	0.44
	KLHL4	C1255G	P419A	0.46
	GPC3	C607T	R203C	0.03
BRx42	PI4KB	G1595A	G532D	0.36
	DSTYK	C1430A	A477D	0.01
	BCL11A	C1595T	A532V	0.65
	INPP4A	C2839A	L947M	0.03
	TTN	T29995G	S9999A	0.50
	CAMK1	C917T	A306V	0.50
	TRIO	C5441T	S1814L	0.55
	PLCG2	C113A	P38H	0.03
	CBFA2T3	G1502T	G501V	0.99
	KDM6B	C417A	S139R	0.99
	MYH1	G2985T	K995N	1.00
BRx61	EPHA10	G928C	E310Q	0.44
	ADAMTSL3	G197C	R66T	0.56
	AFF4	C671T	S224F	0.02
	TTN	C70978T	R23660*	0.49
	TAOK3	G681A	M227I	0.47

a: Allele frequency within cultured CTC cell populations was calculated as the ratio between mutant sequence reads and total reads for each gene.

b: Cases for which DNA from normal tissue were not available

* Denotes chain terminating codon. _splice denotes splice site mutation.

Table S3. List of drugs, targeted pathways, and doses.

		Doses (uM)					
Drugs	**Targeted pathways**						
BYL719	PI3K	0	0.125	0.25	0.5	1	2
Fulvestrant	ER	0	0.0625	0.125	0.25	0.5	1
Everolimus	mTOR	0	0.0625	0.125	0.25	0.5	1
BYL+Fulv.	PI3K+ER	0	0.125+0.0625	0.25+0.125	0.5+0.25	1+0.5	2+1
BYL+Ever.	PI3K+mTOR	0	0.125+0.0625	0.25+0.125	0.5+0.25	1+0.5	2+1
Fulv.+Ever.	ER+mTOR	0	0.0625+0.0625	0.125+0.125	0.25+0.25	0.5+0.5	1+1
LEE-011	CDK4/6	0	0.5	1	2	4	8
PD0332991	CDK4/6	0	0.016	0.032	0.064	0.128	0.256
BYL+LEE011	PI3K+CDK4/6	0	0.125+0.5	0.25+1	0.5+2	1+4	2+8
BYL+PD	PI3K+CDK4/6	0	0.125+0.016	0.25+0.032	0.5+0.064	1+0.128	2+0.256
OSI-906	IGFR	0	0.16	0.32	0.64	1.28	2.56
BMS-754807	IGFR	0	0.16	0.32	0.64	1.28	2.56
BYL+OSI	PI3K+IGFR	0	0.125+0.16	0.25+0.32	0.5+0.64	1+1.28	2+2.56
BYL+BMS	PI3K+IGFR	0	0.125+0.16	0.25+0.32	0.5+0.64	1+1.28	2+2.56
Tamoxifen	ER	0	0.125	0.25	0.5	1	2
Fulvestrant	ER	0	0.0625	0.125	0.25	0.5	1
Raloxifene	ER	0	0.125	0.25	0.5	1	2
Bazedoxifene	ER	0	0.0625	0.125	0.25	0.5	1
Tamo.+Ever.	ER+mTOR	0	0.125+0.0625	0.25+0.125	0.5+0.25	1+0.5	2+1
Fulv.+Ever.	ER+mTOR	0	0.0625+0.0625	0.125+0.125	0.25+0.25	0.5+0.5	1+1
Ralo.+Ever.	ER+mTOR	0	0.125+0.0625	0.25+0.125	0.5+0.25	1+0.5	2+1
Baze.+Ever.	ER+mTOR	0	0.0625+0.0625	0.125+0.125	0.25+0.25	0.5+0.5	1+1
STA9090	HSP90	0	0.016	0.032	0.064	0.128	0.256

Tamo.+STA	ER+HSP90	0	0.125+0.016	0.25+0.032	0.5+0.064	1+0.128	2+0.256
Fulv.+STA	ER+HSP90	0	0.0625+0.016	0.125+0.032	0.25+0.064	0.5+0.128	1+0.256
Ralo.+STA	ER+HSP90	0	0.125+0.016	0.25+0.032	0.5+0.064	1+0.128	2+0.256
Baze.+STA	ER+HSP90	0	0.0625+0.016	0.125+0.032	0.25+0.064	0.5+0.128	1+0.256
BYL+STA	PI3K+HSP90	0	0.125+0.016	0.25+0.032	0.5+0.064	1+0.128	2+0.256
PD173074	FGFR1	0	0.5	1	2	4	8
AZD4547	FGFR2	0	0.05	0.1	0.2	0.4	0.8
BYL+PD	PI3K+FGFR1	0	0.125+0.5	0.25+1	0.5+2	1+4	2+8
BYL+AZD	PI3K+FGFR2	0	0.125+0.05	0.25+0.1	0.5+0.2	1+0.4	2+0.8
Taxol	Chemotherapy	0	0.0064	0.0128	0.0256	0.0512	0.1024
Doxorubicin	Chemotherapy	0	0.05	0.1	0.2	0.4	0.8
Capcitabine	Chemotherapy	0	0.25mM	0.5mM	1mM	2mM	4mM
Olaparib	PARP	0	0.32	0.64	1.28	2.56	5.12
AZD7762	CHK	0	0.0625	0.125	0.25	0.5	1
Olap.+AZD7762	PARP+CHK	0	0.32+0.0625	0.64+0.125	1.28+0.25	2.56+0.5	5.12+1
GSK690693	AKT	0	0.64	1.28	2.56	5.12	10.24
Paclitaxel+GSK.	Chemo.+AKT	0	0.0064+0.64	0.0128+1.28	0.0256+2.56	0.0512+5.12	0.1024+10.24

References and Notes

1. D. A. Haber, N. S. Gray, J. Baselga, The evolving war on cancer. *Cell* **145**, 19–24 (2011). Medline doi:10.1016/j.cell.2011.03.026

2. M. Yu, S. Stott, M. Toner, S. Maheswaran, D. A. Haber, Circulating tumor cells: Approaches to isolation and characterization. *J. Cell Biol.* **192**, 373–382 (2011). Medline doi:10.1083/jcb.201010021

3. E. Ozkumur, A. M. Shah, J. C. Ciciliano, B. L. Emmink, D. T. Miyamoto, E. Brachtel, M. Yu, P. I. Chen, B. Morgan, J. Trautwein, A. Kimura, S. Sengupta, S. L. Stott, N. M. Karabacak, T. A. Barber, J. R. Walsh, K. Smith, P. S. Spuhler, J. P. Sullivan, R. J. Lee, D. T. Ting, X. Luo, A. T. Shaw, A. Bardia, L. V. Sequist, D. N. Louis, S. Maheswaran, R. Kapur, D. A. Haber, M. Toner, Inertial focusing for tumor antigen-dependent and -independent sorting of rare circulating tumor cells. *Sci. Transl. Med.* **5**, 179ra47 (2013). Medline doi:10.1126/scitranslmed.3005616

4. X. Liu, V. Ory, S. Chapman, H. Yuan, C. Albanese, B. Kallakury, O. A. Timofeeva, C. Nealon, A. Dakic, V. Simic, B. R. Haddad, J. S. Rhim, A. Dritschilo, A. Riegel, A. McBride, R. Schlegel, ROCK inhibitor and feeder cells induce the conditional reprogramming of epithelial cells. *Am. J. Pathol.* **180**, 599–607 (2012). Medline doi:10.1016/j.ajpath.2011.10.036

5. T. Sato, H. Clevers, Primary mouse small intestinal epithelial cell cultures. *Methods Mol. Biol.* **945**, 319–328 (2013). Medline doi:10.1007/978-1-62703-125-7_19

6. T. A. Ince, A. L. Richardson, G. W. Bell, M. Saitoh, S. Godar, A. E. Karnoub, J. D. Iglehart, R. A. Weinberg, Transformation of different human breast epithelial cell types leads to distinct tumor phenotypes. *Cancer Cell* **12**, 160–170 (2007). Medline doi:10.1016/j.ccr.2007.06.013

7. J. Debnath, S. K. Muthuswamy, J. S. Brugge, Morphogenesis and oncogenesis of MCF-10A mammary epithelial acini grown in three-dimensional basement membrane cultures. *Methods* **30**, 256–268 (2003). Medline doi:10.1016/S1046-2023(03)00032-X

8. G. Dontu, W. M. Abdallah, J. M. Foley, K. W. Jackson, M. F. Clarke, M. J. Kawamura, M. S. Wicha, In vitro propagation and transcriptional profiling of human mammary stem/progenitor cells. *Genes Dev.* **17**, 1253–1270 (2003). Medline doi:10.1101/gad.1061803

9. D. Dias-Santagata, S. Akhavanfard, S. S. David, K. Vernovsky, G. Kuhlmann, S. L. Boisvert, H. Stubbs, U. McDermott, J. Settleman, E. L. Kwak, J. W. Clark, S. J. Isakoff, L. V. Sequist, J. A. Engelman, T. J. Lynch, D. A. Haber, D. N. Louis, L. W. Ellisen, D. R. Borger, A. J. Iafrate, Rapid targeted mutational analysis of human tumours: A clinical platform to guide personalized cancer medicine. *EMBO Mol. Med.* **2**, 146–158 (2010). Medline doi:10.1002/emmm.201000070

10. M. S. Lawrence, P. Stojanov, C. H. Mermel, J. T. Robinson, L. A. Garraway, T. R. Golub, M. Meyerson, S. B. Gabriel, E. S. Lander, G. Getz, Discovery and saturation analysis of cancer genes across 21 tumour types. *Nature* **505**, 495–501 (2014). Medline doi:10.1038/nature12912

11. Q. X. Zhang, A. Borg, D. M. Wolf, S. Oesterreich, S. A. Fuqua, An estrogen receptor mutant with strong hormone-independent activity from a metastatic breast cancer. *Cancer Res.* **57**, 1244–1249 (1997). Medline

12. D. R. Robinson, Y. M. Wu, P. Vats, F. Su, R. J. Lonigro, X. Cao, S. Kalyana-Sundaram, R. Wang, Y. Ning, L. Hodges, A. Gursky, J. Siddiqui, S. A. Tomlins, S. Roychowdhury, K. J. Pienta, S. Y. Kim, J. S. Roberts, J. M. Rae, C. H. Van Poznak, D. F. Hayes, R. Chugh, L. P. Kunju, M. Talpaz, A. F. Schott, A. M. Chinnaiyan, Activating ESR1 mutations in hormone-resistant metastatic breast cancer. *Nat. Genet.* **45**, 1446–1451 (2013). Medline doi:10.1038/ng.2823

13. W. Toy, Y. Shen, H. Won, B. Green, R. A. Sakr, M. Will, Z. Li, K. Gala, S. Fanning, T. A. King, C. Hudis, D. Chen, T. Taran, G. Hortobagyi, G. Greene, M. Berger, J. Baselga, S. Chandarlapaty, ESR1 ligand-binding domain mutations in hormone-resistant breast cancer. *Nat. Genet.* **45**, 1439–1445 (2013). Medline doi:10.1038/ng.2822

14. S. Li, D. Shen, J. Shao, R. Crowder, W. Liu, A. Prat, X. He, S. Liu, J. Hoog, C. Lu, L. Ding, O. L. Griffith, C. Miller, D. Larson, R. S. Fulton, M. Harrison, T. Mooney, J. F. McMichael, J. Luo, Y. Tao, R. Goncalves, C. Schlosberg, J. F. Hiken, L. Saied, C. Sanchez, T. Giuntoli, C. Bumb, C. Cooper, R. T. Kitchens, A. Lin, C. Phommaly, S. R. Davies, J. Zhang, M. S. Kavuri, D. McEachern, Y. Y. Dong, C. Ma, T. Pluard, M. Naughton, R. Bose, R. Suresh, R. McDowell, L. Michel, R. Aft, W. Gillanders, K. DeSchryver, R. K. Wilson, S. Wang, G. B. Mills, A. Gonzalez-Angulo, J. R. Edwards, C. Maher, C. M. Perou, E. R. Mardis, M. J. Ellis, Endocrine-therapy-resistant ESR1 variants revealed by genomic characterization of breast-cancer-derived xenografts. *Cell Reports* **4**, 1116–1130 (2013). Medline doi:10.1016/j.celrep.2013.08.022

15. K. Merenbakh-Lamin, N. Ben-Baruch, A. Yeheskel, A. Dvir, L. Soussan-Gutman, R. Jeselsohn, R. Yelensky, M. Brown, V. A. Miller, D. Sarid, S. Rizel, B. Klein, T. Rubinek, I. Wolf, D538G mutation in estrogen receptor-α: A novel mechanism for acquired endocrine resistance in breast cancer. *Cancer Res.* **73**, 6856–6864 (2013). Medline doi:10.1158/0008-5472.CAN-13-1197

16. The Cancer Genome Atlas Network, *Nature* **490**, 61 (2012). Medline doi:10.1038/nature11412

17. M. J. Garnett, E. J. Edelman, S. J. Heidorn, C. D. Greenman, A. Dastur, K. W. Lau, P. Greninger, I. R. Thompson, X. Luo, J. Soares, Q. Liu, F. Iorio, D. Surdez, L. Chen, R. J. Milano, G. R. Bignell, A. T. Tam, H. Davies, J. A. Stevenson, S. Barthorpe, S. R. Lutz, F. Kogera, K. Lawrence, A. McLaren-Douglas, X. Mitropoulos, T. Mironenko, H. Thi, L. Richardson, W. Zhou, F. Jewitt, T. Zhang, P. O'Brien, J. L. Boisvert, S. Price, W. Hur, W. Yang, X. Deng, A. Butler, H. G. Choi, J. W. Chang, J. Baselga, I. Stamenkovic, J. A. Engelman, S. V. Sharma, O. Delattre, J. Saez-Rodriguez, N. S. Gray, J. Settleman, P. A. Futreal, D. A. Haber, M. R. Stratton, S. Ramaswamy, U. McDermott, C. H. Benes, Systematic identification of genomic markers of drug sensitivity in cancer cells. *Nature* **483**, 570–575 (2012). Medline doi:10.1038/nature11005

18. K. E. Weis, K. Ekena, J. A. Thomas, G. Lazennec, B. S. Katzenellenbogen, Constitutively active human estrogen receptors containing amino acid substitutions for tyrosine 537 in the receptor protein. *Mol. Endocrinol.* **10**, 1388–1398 (1996). Medline

19. J. Baselga, M. Campone, M. Piccart, H. A. Burris 3rd, H. S. Rugo, T. Sahmoud, S. Noguchi, M. Gnant, K. I. Pritchard, F. Lebrun, J. T. Beck, Y. Ito, D. Yardley, I. Deleu, A. Perez, T. Bachelot, L. Vittori, Z. Xu, P. Mukhopadhyay, D. Lebwohl, G. N. Hortobagyi, Everolimus in postmenopausal hormone-receptor-positive advanced breast cancer. *N. Engl. J. Med.* **366**, 520–529 (2012). Medline doi:10.1056/NEJMoa1109653

20. Y. Wang, J. B. Trepel, L. M. Neckers, G. Giaccone, STA-9090, a small-molecule Hsp90 inhibitor for the potential treatment of cancer. *Curr. Opin. Investig. Drugs* **11**, 1466–1476 (2010). Medline

21. P. Furet, V. Guagnano, R. A. Fairhurst, P. Imbach-Weese, I. Bruce, M. Knapp, C. Fritsch, F. Blasco, J. Blanz, R. Aichholz, J. Hamon, D. Fabbro, G. Caravatti, Discovery of NVP-BYL719 a potent and selective phosphatidylinositol-3 kinase alpha inhibitor selected for clinical evaluation. *Bioorg. Med. Chem. Lett.* **23**, 3741–3748 (2013). Medline doi:10.1016/j.bmcl.2013.05.007

22. P. R. Gavine, L. Mooney, E. Kilgour, A. P. Thomas, K. Al-Kadhimi, S. Beck, C. Rooney, T. Coleman, D. Baker, M. J. Mellor, A. N. Brooks, T. Klinowska, AZD4547: An orally bioavailable, potent, and selective inhibitor of the fibroblast growth factor receptor tyrosine kinase family. *Cancer Res.* **72**, 2045–2056 (2012). Medline doi:10.1158/0008-5472.CAN-11-3034

23. M. Mohammadi, S. Froum, J. M. Hamby, M. C. Schroeder, R. L. Panek, G. H. Lu, A. V. Eliseenkova, D. Green, J. Schlessinger, S. R. Hubbard, Crystal structure of an angiogenesis inhibitor bound to the FGF receptor tyrosine kinase domain. *EMBO J.* **17**, 5896–5904 (1998). Medline doi:10.1093/emboj/17.20.5896

24. M. Pollak, The insulin and insulin-like growth factor receptor family in neoplasia: An update. *Nat. Rev. Cancer* **12**, 159–169 (2012). Medline

25. I. Baccelli, A. Schneeweiss, S. Riethdorf, A. Stenzinger, A. Schillert, V. Vogel, C. Klein, M. Saini, T. Bäuerle, M. Wallwiener, T. Holland-Letz, T. Höfner, M. Sprick, M. Scharpff, F. Marmé, H. P. Sinn, K. Pantel, W. Weichert, A. Trumpp, Identification of a population of blood circulating tumor cells from breast cancer patients that initiates metastasis in a xenograft assay. *Nat. Biotechnol.* **31**, 539–544 (2013). Medline doi:10.1038/nbt.2576

26. L. Zhang, L. D. Ridgway, M. D. Wetzel, J. Ngo, W. Yin, D. Kumar, J. C. Goodman, M. D. Groves, D. Marchetti, The identification and characterization of breast cancer CTCs competent for brain metastasis. *Sci. Transl. Med.* **5**, 180ra48 (2013). Medline doi:10.1126/scitranslmed.3005109

27. N. M. Karabacak, P. S. Spuhler, F. Fachin, E. J. Lim, V. Pai, E. Ozkumur, J. M. Martel, N. Kojic, K. Smith, P. I. Chen, J. Yang, H. Hwang, B. Morgan, J. Trautwein, T. A. Barber, S. L. Stott, S. Maheswaran, R. Kapur, D. A. Haber, M. Toner, Microfluidic, marker-free isolation of circulating tumor cells from blood samples. *Nat. Protoc.* **9**, 694–710 (2014). Medline doi:10.1038/nprot.2014.044

28. J. Lee, J. B. Wang, F. Bersani, B. Parekkadan, Capture and printing of fixed stromal cell membranes for bioactive display on PDMS surfaces. *Langmuir* **29**, 10611–10616 (2013). Medline doi:10.1021/la4012795

29. K. Cibulskis, M. S. Lawrence, S. L. Carter, A. Sivachenko, D. Jaffe, C. Sougnez, S. Gabriel, M. Meyerson, E. S. Lander, G. Getz, Sensitive detection of somatic point mutations in impure and heterogeneous cancer samples. *Nat. Biotechnol.* **31**, 213–219 (2013). Medline doi:10.1038/nbt.2514

30. D. A. Barbie, P. Tamayo, J. S. Boehm, S. Y. Kim, S. E. Moody, I. F. Dunn, A. C. Schinzel, P. Sandy, E. Meylan, C. Scholl, S. Fröhling, E. M. Chan, M. L. Sos, K. Michel, C. Mermel, S. J. Silver, B. A. Weir, J. H. Reiling, Q. Sheng, P. B. Gupta, R. C. Wadlow, H. Le, S. Hoersch, B. S. Wittner, S. Ramaswamy, D. M. Livingston, D. M. Sabatini, M. Meyerson, R. K. Thomas, E. S. Lander, J. P. Mesirov, D. E. Root, D. G. Gilliland, T. Jacks, W. C. Hahn, Systematic RNA interference reveals that oncogenic KRAS-driven cancers require TBK1. *Nature* **462**, 108–112 (2009). Medline doi:10.1038/nature08460